Carla Sofia Gonçalves Martins

Licenciado em Ciências de Engenharia de Micro e Nanotecnologias

Optimization of Printed TIPS-Pentacene Thin-Film Applied on OFET technology

Dissertation submitted in partial fulfillment
of the requirements for the degree of

Master of Science in
Micro and Nanotechnologies Engineering

Adviser: Roberto Mendonça Faria, Full Professor, University of São Paulo

Co-adviser: Elvira Maria Correia Fortunato, Full Professor, NOVA University of Lisbon

Examination Committee

Chairperson: Rodrigo Ferrão de Paiva Martins
Raporteurs: Luís Miguel Nunes Pereira
Members: Elvira Maria Correia Fortunato

FACULDADE DE CIÊNCIAS E TECNOLOGIA
UNIVERSIDADE NOVA DE LISBOA

DRAFT: January 2, 2017

Optimization of Printed TIPS-Pentacene Thin-Film Applied on OFET technology

This document was created using the (pdf)LaTeX processor, based in the "unlthesis" template[1], developed at the Dep. Informática of FCT-NOVA [2].
[1] https://github.com/joaomlourenco/unlthesis [2] http://www.di.fct.unl.pt

Acknowledgements

Gostaria de começar por agradecer ao meu orientador, o Professor Dr. Roberto Faria, que me recebeu e orientou na Universidade de São Paulo e cujo apoio, dedicação e entusiasmo pela área fizeram toda a diferença ao longo dos vários momentos que constituíram esta fase. Um grande obrigado por tudo do fundo do coração. À minha orientadora da FCT-UNL, Prof. Dra. Elvira Fortunato, que me proporcionou a oportunidade de ir para a USP realizar este trabalho e que cujo apoio em todo o processo foi indispensável.

Aos meus pais, Belém e Emília, a quem dedico esta tese, pelo apoio imprescindível em todos os desafios a que me proponho. Devo a vocês a mulher que sou hoje. Ter conseguido atingir esta meta teria sido impossível sem a vossa dedicação incansável ao longo dos meus 23 anos. As palavras faltam-me para agradecer tudo que me têm proporcionado.

Quero agradecer também aos meus irmãos, Joel e Henrique, por todas as brigas e reconciliações, e por sempre me tratarem como uma eterna criança e assim me lembrarem que sempre serei a menina dos vossos olhos.

Ao meu Dioguinho , o meu sobrinho afilhado preferido, por me encher de amor e de mimo. Por me chamar de tia querida e me abraçar todas as vezes com tanta convicção e carinho.

A toda a família do Prof. Faria em especial à Julia, a minha irmã de coração, por me ter recebido de braços abertos no Brasil. Por todos os momentos incríveis passados em São Paulo. Por todas as risadas e lágrimas, viagens e momentos de introspetiva, muito obrigada super mulher.

A todas as pessoas do Grupo de Polímeros do Instituto de Física da USP que me ajudaram na transição e me receberam como um deles em especial à Josiani pela orientação com o equipamento Microdrop assim como com todo o procedimento realizado. Sem você e o seu conhecimento não teria atingido os resultados obtidos. Obrigada Josi.

À Simone da secretaria do Grupo de Polímeros que sempre foi impecável quando precisei de ajuda com qualquer assunto. Por todos os bom dias no grupo com um sorriso lindo na cara um muito obrigado.

Ao Prof. Dr. Rodrigo Martins e à Prof. Dra. Elvira Fortunato pela criação, promoção e reconhecimento alcançado pelo curso de Engenharia de Micro e Nanotecnologias.

À Moura, por todas as conversas, risadas, brigas, momentos partilhados ao longo de todos estes anos, mas principalmente pela cumplicidade e amizade à distância que nunca imaginei perdorar deste jeito um muito obrigada. Espero ter-te para sempre comigo.

Às minhas gatas de Barcelos, Mariana, Kika, Marta, Cláudia, Bea, Zé, Nokas e Driz por todos estes anos de companheirismo, partilha, de risadas, parvoíces, mas principalmente por sempre me apoiarem em todas as decisões que venho a tomar e sempre me receberem de volta a casa de braços abertos com um sorriso na cara. Posso ir onde for, posso demorar o tempo que demorar que sempre vos carrego comigo no coração. Todas as cidades do mundo seriam fáceis de viver por tempo ilimitado se vos tivesse ao meu lado. Um livro não chegava para explicar a importância destas mulheres na minha vida. Cada uma ao seu jeito faz de mim uma pessoa melhor. Dos maiores orgulhos que tenho nesta vida é poder chamar-vos de amigas. Obrigada por tudo manas pé na porta!

Ao meu Mano Cristiano por sempre me acompanhar nas aventuras, por ter sempre uma palavra motivadora a dar, assim como por me fazer rir a toda a hora, um muito obrigada!

Aos meus padrinhos da faculdade, Bea e Daniel, por me terem guiado desde o primeiro dia da faculdade, por nunca me terem deixado sentir sozinha em Lisboa, por me terem apoiado, aconselhado, rido e vivido toda a experiência que foi estudar na FCT ao meu lado. Hoje ainda com mais certeza posso afirmar que escolhi os melhores padrinhos do mundo. Muito obrigada!

Aos meus camaradas, companheiros de curso, Bártolo, Francisco, Correia, Luka, Trigo, Monteiro e Tomás quero agradecer todas as experiências vividas e partilhadas ao longo destes anos. Sei que poderei contar com vocês para sempre. Espero sempre ter este grupinho por perto com a sua boa disposição para animar os meus dias.

À alfacinha da Joana Machado por todo o carinho e pela amizade tão bem regada ao longo destes cinco anos. Espero sempre ter-te na minha vida, a aconselhar, acompanhar e partilhar tudo que a vida terá para nos oferecer.

À Sabala por estar sempre lá quando eu preciso. Seja dia seja noite, faça chuva ou faça sol sei que posso sempre contar contigo. Obrigada por todos os conselhos, risadas, jantaradas e noitadas. Estás sempre lá, e sem muitos floreados, és a mana da margem sul que todos precisavam de ter na vida. Obrigada chavala.

Aos meus afilhados, Alexandra, Cátia, Viorel, Fernandes, André, Miguel e Sérgio, com especial atenção a este último caloirito que é muito mais que um afilhado, um grande amigo que sempre esteve lá nos bons e maus momentos do meu mestrado, e que tenho um orgulho enorme no homem com H grande em que se tornou.

Ao Zé, por todo o companheirismo ao longo destes cinco anos, pela partilha, pela amizade, pela boa disposição, e noitadas. Este senhor sempre me ensinou e guiou ao longo do meu percurso na Caparica e a ele devo grande parte do meu sucesso académico. Um muito obrigada. Tenho muito orgulho em ter-te como amigo. Fico aqui para assitir ao teu sucesso e aplaudir-te hoje e sempre.

Ao Jaime por todo o apoio incansável a toda a hora do dia e da noite e pelos abraços apertados em horas de stress. É das pessoas que mais me surpreendeu ao longo do curso e que mais falta me faz pela boa energia que sempre me fez sentir. Toda a gente precisa dum Jaime como este nas suas vidas. Obrigada coração

À Fernanda e ao Carlos, por tudo que fizeram por mim no Brasil. Sem me conhecerem, receberam-me em vossa casa em São Paulo sempre de bom grado e partilharam o vosso espaço comigo. Vocês foram os Portugueses no Brasil que me apoiaram e me ajudaram a matar as saudades do sotaque mais lindo de Portugal, o do Norte! Por todos os fins de semana a passear por SP, pelas risadas, pela boa disposição e pelas loucuras, um muito obrigada! Ficarão para sempre no meu coração e sempre terão a porta de minha casa aberta.

À Naiara, a minha parceira da maldade de São Carlos um muito obrigada! Obrigada por todas as risadas, cumplicidade, pelas loucuras, conversas pela noite dentro e por me

teres recebido em tua casa de braços abertos de um jeito que eu nunca esquecerei. Espero ver-te em breve amiga, fazes falta.

Ao Giácomo por seres a pessoa linda que és. Por todas as risadas, loucuras e brincadeiras um muito obrigada. Em tão pouco tempo conseguis-te deixar marca na minha vida, e entras-te no meu coração para ficar. O mundo precisa de mais homens como você.

Ao André, à Isabella, à Ana, às meninas da República Saia Jeans, à Bárbara, à Luciana, aos meninos da Nossa Rep, e a todo o mundo de São Carlos, SP, que me recebeu e me marcou um muito obrigada! Espero que a gente um dia se volte a encontrar.

Aos ex-basolhences, Jacinto, Diogo, Júlio, Rosado e Coelho, por todas as noitadas, risadas partilhadas, por toda a vossa estupidez colectiva e principalmente pela vossa amizade incondicional.

Ao Conselho de Praxe da FCT pela união, trabalho em equipa e companheirismo. A praxe fez de mim uma pessoa melhor, devo a ela a maioria dos amigos que fiz na faculdade e a vossas devo o reconhecimento por todo o amor e dedicação ao espírito académico.

Às minhas cadelas Lua, Mimi e à pequena Clarinha um muito obrigada. O amor que elas me dão todos os dias faz de mim uma pessoa melhor.

A todas as pessoas do curso de MIEMN, aos que frequentam a 202 e a todos os que, de alguma forma, contribuíram para que me tornasse na pessoa que sou hoje e que não foram mencionadas em cima.

"The distance between insanity and genius is measured only by success."
Bruce Feirstein

Abstract

The area of Printed Electronics is relatively new, but promises to make a revolution in several applications, particularly in smart cards and radio-frequency identification devices (RFIDs). However, to achieve this goal is of fundamental importance to progress towards printed transistors and complementary circuits. In this sense, this thesis aims to advance the research on printing Organic Field-Effect Transistors (OFETs), both p-type and n-type. The first step was to dominate the processing technique of thin films composed by TIPS-Pentacene (a p-type molecule), as well as to adjust the parameters of its solution to produce suitable electronic ink for inkjet printing. Other important step was to treat the surface dielectric layer, which is as important as the semiconductor layer for a good performance of an OFET. We choose poly(methyl metacrilate) (PMMA) as the insulator material. A detailed study of the morphology of printed TIPS-Pentacene was also carried out. After the deposition of the dielectric and the semiconductor layers, which showed good crystallinity index, we characterized the p-OFET and built a pMOS inverter, which shows to be promising in logical circuits. With these results in mind, the next step is to build a CMOS inverter-TIPS Pentacene / P(NDI2OD-T2) and thus pave the way for the manufacture of a complementary circuit.

Keywords: OFET, Inkjet, TIPS-Pentacene,Printed Electronics, SAM, HMDS

Resumo

A área de Eletrónica Impressa é relativamente nova, mas promete revolucionar vários setores sobretudo o de cartões inteligentes e de dispositivos de identificação por radio frequência (RFIDs – Radio Frequency Identifications). No entanto, para tal é de fundamental importância o domínio da fabricação de transistores impressos e de circuitos complementares. Neste sentido, esta tese tem como objetivo avançar nas pesquisas relativas à impressão de transistores orgânicos por efeito de campo (OFETs – Organic Field-Effect Transistors), tanto tipo p como tipo n. O primeiro passo foi dominar o processamento de filmes finos compostos por TIPS-Pentaceno (molécula do tipo-p), assim como ajustar os parâmetros da sua solução de modo a tornar-se numa tinta adequada à impressão pela técnica Inkjet. Outro passo importante foi tratar a superfície da camada dielétrica, que é tão importante quanto a camada semicondutora para o bom funcionamento de um OFET. Usou-se o polimetracrilato de metila (PMMA) como material isolante. Um estudo detalhado da morfologia do TIPS-Pentaceno impresso foi também realizado. Após a deposição do dielétrico e da camada semiconductora, que apresentou um bom índice de cristalinidade , caracterizou-se o p-OFET e construiu-se um inversor pMOS, que demonstra ser um conceito promissor para os circuitos lógicos. Tendo em conta os resultados, o próximo passo é construir um inversor CMOS TIPS-Pentacene/P(NDI2OD-T2) e assim abrir caminho para a produção de circuitos complementares.

Palavras-chave: OFET, Inkjet, TIPS-Pentaceno, Eletrónica Impressa, SAM, HMDS

Contents

List of Figures xvii

List of Tables xix

Symbols xxi

Abreviations xxiii

Motivation xxv

1 Introduction 1
- 1.1 The Organic Field Effect Transistor (OFET) . . . 1
  - 1.1.1 Basic OFET Operation . . . 1
  - 1.1.2 Carrier Transport Phenomenon . . . 3
- 1.2 Inkjet Printing . . . 4
  - 1.2.1 Drying Process . . . 5

2 Materials 7
- 2.1 Organic Semiconductor-TIPS-Pentacene . . . 7

3 Experimental 9
- 3.1 Devices Fabrication . . . 9
- 3.2 Inkjet Printing Semiconductor Process . . . 10

4 Analyse of the Dielectric and Active Layer 11
- 4.1 Device's Architecture . . . 11
- 4.2 Dielectric Layer . . . 11
  - 4.2.1 Dielectric/semiconductor Interface Treatment . . . 12
- 4.3 Semiconductor Layer . . . 14
  - 4.3.1 Semiconductor Solvent . . . 14
  - 4.3.2 Printed Parameters for Semiconductor Layer . . . 15
- 4.4 Structure and Morphology of the Printed Layers . . . 17
  - 4.4.1 Images of Scanning Electron Microscope . . . 17
  - 4.4.2 Wide-Angle X-ray Diffraction . . . 18

5 OFETs and Inverter 21
  - 5.0.1 OFETs: Drain current (I_D) versus source-drain voltage (V_D) . . . 21
- 5.1 p-OFETs-tetralin . . . 22
- 5.2 Inverter Characterization . . . 23
- 5.3 n-OFET . . . 24

6 Conclusions and Final Remarks 27

Bibliography 29

A Electrical Characterization of OFETs **35**

List of Figures

1.1 (a) Scheme of an OFET type Bottom Gate-Top Contact;(b) Correspondent electronic structure (adapted from [14]) . . . 1
1.2 Operation regimes of Organic Field Effect Transistors (OFETs): (a) linear regime; (b) pinch-off e (c) saturation regime. . . . 2
1.3 (a)Overlapping p_z orbitals of the conjugated segment(Adapted from [23]); (b) Illustration of bonding and antibonding interactions between HOMO and LUMO levels . . . 4
1.4 Printable lines: (a) individual drops, (b) scalloped, (c) uniform, (d) with bumps (bulges), and (e) stacked coins.(Adapted from [28]) . . . 5
1.5 Solvent evaporation during the drying process (Inspired by [29]) . . . 5

2.1 Molecular and stacking structure of pentacene (a and c) and of TIPS-Pentacene (b and d, respectively). This figure has adapted from [30, 31] . . . 7

3.1 Schematic showing the process to obtain a OFET from a glass substrate previously clean (a), following to thermal evaporation of the gate (b), spin-coated dielectric film (c) leading to its surface treatment with UVO Radiation (d) and spontaneous evaporation of Self Assembled Monolayer (SAM) (e), deposition of the TIPS-Pentacene by Inkjet Printer(f), and thermal evaporation of the source and drain contacts (g) respectively. . . . 9
3.2 shadow masks used for evaporation of the contacts source/drain (left) and gate (right) . . . 10
3.3 Printer Autodrop. Printer Overview (a) and expansion of the area highlighted in green showing printing system (b) Drop Formation of the TIPS Pentacene (c) . . . 10

4.1 Root-mean-square (RMS) roughness of PMMA (a) without treatment; (b) with 7s UVO treatment . . . 13
4.2 The results of XRD spectroscopy of different TIPS-Pentacene solvents with (b and d) and whithout (a and c) HMDS monolayer . . . 14
4.3 Structural formula of: (a) tetralin, and (b) anisole . . . 15
4.4 Printed TIPS-Pentacene/Anisole lines with different values of spacing drops 16
4.5 Coffee Ring Effect . . . 16
4.6 Crystalline structures formed in printed (a) TIPS-Pentacene/Anisole lines to 250 μm spacing drops and (b) TIPS-Pentacene/Tetralin lines to 330 μm spacing drops . . . 17
4.7 Analyzed SEM image and crystalization of an thin films formed by drop casting technique . . . 18
4.8 Analyzed SEM image and crystalization of an thin films formed by inkjet printing . . . 18
4.9 WAXD obtained from: a) nude glass substrate; and b) the same substrate coated with PMMA functionalized with HMDS. . . . 19

4.10 WADX obtained from TIPS-pentacene film deposited by: a)inkjet printing on the substrate coated with PMMA functionalized with HMDS; b)drop casting 19

5.1 Drain current vs Drain-source voltage of p-OFETs: a) TIPS-pentacene dissolved in Anisole; b) TIPS-pentacene dissolved in Tetraline 21
5.2 Characteristic curves of a p-OFET printed at 36°C: (a) $I_D - V_D$ curve; (b) $I_D - V_G$ transfer characteristic; and (c) $(I_D.L/W)^2$ x V_G and $Log(I_D.L/W)$ x V_G curves. 22
5.3 Characteristic curves of a p-OFET printed at 46°C: (a) $I_D - V_D$ curve; (b) $I_D - V_G$ transfer characteristic; and (c) $(I_D.L/W)^2$ x V_G and $Log(I_D.L/W)$ x V_G curves. 23
5.4 PMOS inverter with a resistor load 23
5.5 Curves of voltage transfer characteristics of the digital inverter. (a) Effect of resistance for $V_{DD} = 60V$; (b) Effect of variation of tension for R=300MΩ; (c) Voltage Transfer Characteristic (VTC) curve with drive voltage gain for $V_{DD} = 60V$ and R=300MΩ 24
5.6 Molecular structure of P(NDI2OD-T2) 25
5.7 Characteristic curves of a n-OFET: (a) $I_D - V_D$ curve; (b) $I_D - V_G$ transfer characteristic; and (c) $(I_D.L/W)^2$ x V_G and $Log(I_D.L/W)$ x V_G curves.) 25

A.1 Representative current-voltage characterisctics of an p-channel organic field-effect transistor. (a) output characteristics;(b) transfer characteristics in the linear regime indicating the onset voltage V_{on} when drain current increases suddenly; (c) transfer characteristics in the saturation regime indicating the threshold voltage V_{th}. This figure has adapted of the [50] 35

List of Tables

4.1 Parameters used to optimize the printing TIPS-Pentacene/Tetralin and TIPS-Pentacene/Anisole 15

5.1 Parameters obtained for p-OFETs (TIPS-Pentacene with tetralin) heated at 36°C during the printing procedure. 22
5.2 Parameters obtained for p-OFETs (TIPS-Pentacene with tetralin) heated at 46°C during the printing procedure. 23
5.3 Truth Table 24
5.4 Parameters obtained for n-OFETs 25

Symbols

σ	Conductivity
π	π molecular orbital
ν	Viscosity of the fluid
γ	Surface tension
ρ	Mass density
μ_{OFET}	Charge carrier mobility
I_D	Drain current
I_{ON}/I_{OFF}	Current ratio
Oh	Ohnesorge Number
V_D	Drain voltage
V_G	Gate voltage
V_{th}	Threshold voltage
p_z	p_z molecular orbital
sp^2	sp^2 atomic orbital
C	Capacitance of dielectric
d	Diameter of the drop
E	Electric field
J	Current density
L	Lenght of the transistor
S	Subthreshold swing

W	Width of the transistor

Abreviations

BG/TC	Bottom Gate/Top Contact
CIJ	Continuous Inkjet Printing
CVD	Chemical Vapor Deposition
DoD	Drop on Demand
FET	Field Effect Transistor
HMDS	Hexamethyldisilazane
HOMO	Highest Occupied Molecular Orbital
LUMO	Lowest Unoccupied Molecular Orbital
nBA	Butyl acrylate
OFET	Organic Field Effect Transistor
OSC	Organic Semiconductor
OTFT	Organic Thin Film Transistor
PMMA	Poly(methyl methacrylate)
PVP	Poly(vinylpyrrolidinone)
RMS	Root-mean-square
SAM	Self Assembled Monolayer
SEM	Scanning Electron Microscope
TIPS-Pentacene	6,13-Bis(triisopropylsilylethynyl)pentacene
UVO	Ultraviolet Ozone
VTC	Voltage Transfer Characteristic
WAXD	Wide-Angle X-ray Diffraction

XRD	X Ray Diffraction

Motivation

Organic semiconductor thin films have open a new branch in electronics that can be named by "Wet Electronics". This denomination, which sounds freak, defines precisely the fact that organic electronics allows the manufacture of devices from an electronic ink. This means that from an appropriate electronic ink it is possible to design and print numerous electronic devices and circuits, by making use of several techniques that have been developed recently. In our case an electronic ink is nothing more than a solution of conjugated organic molecules in organic solvents. Important advantages are them derived as their adaptability to low-temperature processing on flexible substrates, low cost processing, amenability to high-speed fabrication, low consumption of inputs, and tunable electronic properties. Such features open possibilities for a variety of next-generation electronic products, including circuits for smart cards, lowpower flexible displays, flexible radio frequency identification (RFID) tags, light panels, and printable sensors, among many other applications [1–4]. The success of printed electronics depends on overcoming the difficulties faced today in the control of printing techniques as well as in the creation of new materials adequate to the preparation of electronic inks. In the specific case of transistors, p-channel molecules are so far the leading class of organic semiconductors. In contrast, n-type molecules are still relatively rare, but they are of great relevance for the development of printed electronic devices such as OFETs. The scope of printed electronics includes a set of printing methods that has been developed to print electronic and optoelectronic devices as well as circuitries on rigid and flexible substrates. The most known techniques used for printed electronics are: screen printing, flexography, rotogravure, offset lithography, and inkjet. Among them, one of the most suitable to print devices in the micrometer scale is the Inkjet technique, mainly to print transistors and complementary circuits [5, 6].

In this sense, this thesis intended to develop a work using inkjet printing to fabricate organic field effect transistors (OFETs) with the objective to contribute to the printed circuits area. We got this objective by the fabrication and characterization of p-OFETs end with the first steps in the fabrication of n-OFETs.

Chapter 1

Introduction

1.1 The Organic Field Effect Transistor (OFET)

OFETs, having a thin film as active layer, are particularly interesting mainly because their fabrication processing are much less complex when compared with conventional Si technology. While Si-technology involves high-temperature and high-vacuum deposition processes associated with sophisticated photolithographic patterning methods, organic electronics can be processed by easy deposition techniques using ordinary organic solutions. In addition, the mechanical flexibility of organic thin films makes them naturally compatible with plastic substrates for lightweight and foldable products. Although OFETs are not meant to replace conventional inorganic transistors – because of the upper limit of their switching speed – they have great potential for a wide variety of applications, especially for new products that rely on their unique characteristics, such as electronic newspapers, inexpensive smart tags for inventory control, and large-area flexible displays. Since the coinage of the first OFET in 1986 [7], the performance of this type of device has greatly progressed, as has been shown by several papers and reviews [8–15].Several applications based on OFETs have been then created and refined, for example: in Light-Emitting Field-Effect Transistor [16, 17], Flexible circuits [18], Optical displays [19], gas sensors [20], and bioelectronics [21].

1.1.1 Basic OFET Operation

OFETs exhibit a similar architecture to the Field Effect Transistors (FETs), i. e. they have three electrodes (source, drain and gate), a semiconductor channel between the source and the drain (which is isolated from the gate by a dielectric layer) as shown in the Figure 1.1(a). Figure 1.1(b) depicts the correspondent electronic structure of an OFET. The basic principle of a FET consists of the modulation of the electric current flowing between the source and the drain by the gate voltage.

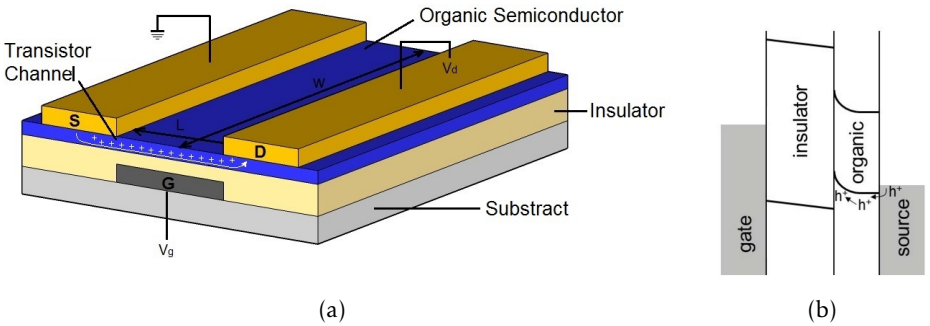

Figure 1.1: (a) Scheme of an OFET type Bottom Gate-Top Contact;(b) Correspondent electronic structure (adapted from [14])

OFET operates in the accumulation mode, as shown in Figure 1.2 (a). At low electric

fields, the transistor operates in an ohmic regime (Figure 1.2 (a)); however as the source-drain voltage increases, the pinch-off phenomenon is reached (Figure 1.2 (b)), in which the electrical characteristic changes from the linear regime to the saturation one (Figure 1.2 (c)).

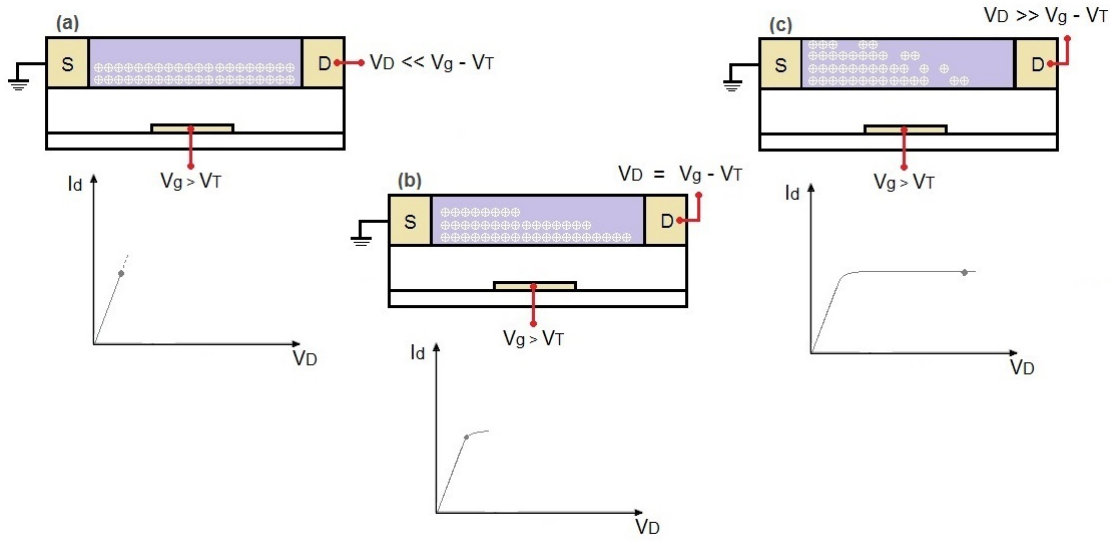

Figure 1.2: Operation regimes of OFETs: (a) linear regime; (b) pinch-off e (c) saturation regime.

The ideal current-voltage curve of a FET in the nonsaturated region is given by the equation:

$$I_D = \frac{WC\mu_{OFET}}{2L}[2(V_G - V_{th})V_D - V_D^2]. \tag{1.1}$$

Where V_G is the voltage between the electrodes gate and source, V_D that between the electrodes drain and source, and V_{th} the threshold voltage. W is the width of the transistor, L the lenght of the channel (see W and L in 1.1(a)), μ_{OFET} the charge carrier mobility, and C the capacitance of the dielectric layer.[22] In the saturation regime, on the other hand, the relation for $V_G > V_{th}$ is described by:

$$I_D = \frac{WC\mu_{SAT}}{2L}(V_G - V_{th})^2 \tag{1.2}$$

It is important to remark that while the capacitance C and the charge carrier mobility μ_{OFET} are essential parameters to govern the performance of the transistor, the W/L is the geometric ratio that defines its current-voltage characteristic.

As in traditional inorganic semiconductors, organic materials can function either as p-type or n-type. In p-type semiconductors the majority carriers are holes, while in n-type the majority carriers are electrons. Until recently, the most widely studied organic semiconductors have been p-type. However, the great effort carried out by organic chemistry has created n-type semiconductor molecules, paving the way to built n-type OFETs.[22] However, since the goal of this work is to develop a fabrication of OFETs

making use of printing methods by specific technique known by Inkjet, we limit ourselves to p-type transistors.

1.1.2 Carrier Transport Phenomenon

As already mentioned above OFETs are usually unipolar devices and operate in the accumulation regime, as shown in the sketches of Figure 1.2. It is important to note that for a perfect operation, the source electrode has to be a blocking contact while the drain electrode should collect the incoming charge carriers without any obstacle. In the linear regime, along the channel, the Ohm's law is obeyed, i. e.,

$$J = E\sigma \tag{1.3}$$

where J is the current density, σ the conductivity and E the electric field established between the source and drain electrodes. It is important to emphasize that the electric field, even for the highest used voltages, does not exceed the value of 100 KV/cm, which discards any effect of the field on the channel conductivity. In order to reach such value the channel length would have a length below 1 μm. On the other hand, the channel conductivity depends on the chemical features of the organic molecule and on the morphological structure of the thin film.

Organic Semiconductors (OSCs) are carbon-based compounds that exhibit a special configuration from which semiconducting properties are derived. Their backbone is based on carbon-hydrogen and invariably presents an alternate sequence of single and double bonds. The semiconductor properties are possible because carbon atoms can form three sp^2 hybridized orbitals (one the molecular plan) and one unhybridized orbital, which is commonly denoted as p_z orbital (one the perpendicular plane to the sp^2 orbitals). This type of hybridization allows the formation of three high energy σ bonds (one per each hybridized orbital) and two π bonds of low energy (one π bond and one antibond π^*). This orbital configuration creates a large energy difference between the occupied bond π or the Highest Occupied Molecular Orbital (HOMO), and the unoccupied bond π^* or the Lowest Unoccupied Molecular Orbital (LUMO) (Figure 1.3(b)). Unhybridized orbitals p_z provide electron clouds above and below the molecular plain. The adjacent p_z orbitals overlap resulting in shared molecular orbitals that are often referred as extended π-system (see Figure 1.3(a)). Electrons on these orbitals are spatially delocalized, meaning that they belong to the whole π-system, but not to specific carbon atoms. A π- system can be extended over the entire organic molecule or just over a conjugated segment. [23–25]

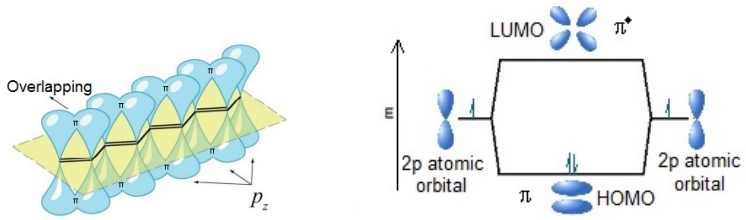

(a) (b)

Figure 1.3: (a)Overlapping p_z orbitals of the conjugated segment(Adapted from [23]); (b) Illustration of bonding and antibonding interactions between HOMO and LUMO levels

1.2 Inkjet Printing

Inkjet printing technology encompasses a wide range of digitally controlled formation of small liquid drops and its deposition on solid and flexible substrates. This technology is usually classified as either Continuous Inkjet Printing (CIJ) or Drop on Demand (DoD) printing: the two are distinguished by the physical process by which the drops are generated.

The operation of an inkjet printer is composed by several steps. The process is initiated by the digitally controlled ejection of tiny drops by a print head onto a substrate. In the case of DoD technology, which is used in this thesis, the drops are formed by the creation of a pressure pulse that can be, in some printers, given by a piezoelectric system. In the Autodrop printer used in this work (Figure 3.3), the operation core is composed by a glass capillary with a nozzle at one end and surrounded by a piezoelectric tube. The capillary is filled with liquid ink. Applying a voltage pulse to the electrodes of the piezo actuator makes it contract and creates the shock wave in the liquid. In general, the nozzle size can be set between 30 and 100 µm.[26]

Surface tension and viscosity are two important parameters that play key essential roles in the formation and behaviour of liquid jets and drops. The flow of a jet emerging from a nozzle is related to the value of the Ohnesorge Number (Oh), which depends on the physico-chemical properties of the liquid and the size scale of the ejected drops and given by the equation:

$$Oh = \frac{\nu}{\sqrt{d\gamma\rho}} \tag{1.4}$$

where ν is the viscosity of the fluid, γ is the surface tension, ρ is the mass density, and d is a characteristic value related to the diameter of the drop. [27]

Since in our work is required the overlapping of droplets to form a continuous pattern characteristic, we need to obtain uniform printed lines. Figure 1.4 exhibits five of the most common five patterns obtained in DoD printing. Certainly, our challenge is to print lines having uniform shape. This is possible by directly controlling the nature of the interaction between the ink and substrate. [28]

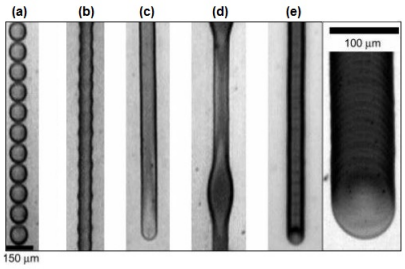

Figure 1.4: Printable lines: (a) individual drops, (b) scalloped, (c) uniform, (d) with bumps (bulges), and (e) stacked coins.(Adapted from [28])

1.2.1 Drying Process

Carrier transport in organic electronic devices is tightly related to the morphology of thin films, which are the active layer of the most part of such devices. Thereby, crystalline microstructures embedded in disordered structures determine the electric properties and therefore the devices performance. Similar situation is faced by printed circuits, in which the final structure of the printed thin film is established by interactions between the organic molecules with the substrate and also depends on the evaporation rate of the solvent. Therefore, the substrate surface energy and the solvent volatibility are important parameters to be defined with precision. In the case of printing devices by inkjet technique, one should also take into account the jetting parameters, which are specific for each type of machine. In conclusion, to print an organic transistor several steps have to be followed with great accuracy to achieve an adequate dried film.

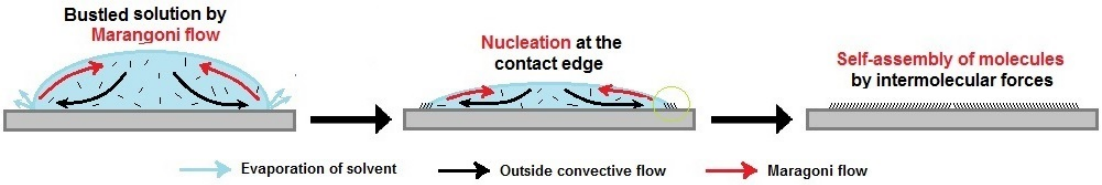

Figure 1.5: Solvent evaporation during the drying process (Inspired by [29])

As the evaporation behavior during the drying process plays an important function in controlling the film morphology, the distribution of droplets in ink-jet printed is of crucial importance to determine the film uniformity. Crystalline structures can be produced using ink-jet printing as a result of the recirculation flows in printed droplets, being induced by the Marangoni flow in a direction counter to the convective flow.

At the beginning the contact line is pinned. Evaporation occurs over the entire drop surface, but its strength has a downwards trend from the edge to the center, as shown in figure 1.5. The Marangoni flow is directed from the edge to the center to compensate for the loss of volume. This drop drying process may give rise to coffee-ring effect. Therefore, one approach to improving the homogeneity of ink-jet-printed deposits involves a high control of all parameters of this technique that play a central role to device performance.[27, 29]

Chapter 2

Materials

2.1 Organic Semiconductor-TIPS-Pentacene

Pentacene is an organic semiconductor small molecule consisting of five linearly-fused benzene rings, as shown in Figure 2.1(a), and it has been extensively used in organic electronic devices, mainly in OFETs [32].Although Pentacene is the most commonly used material in organic electronic devices, this compound has two great disadvantages:: (i) a poor overlap between HOMO orbitals, which results in relatively low charge carrier mobility; ii) it is insoluble in many common organic solvents, and when in solution is subject to photo-dimerization. The low mobility comes from the fact that it forms a herringbone crystal structure in which each acene backbone is positioned nearly perpendicular to its neighbor pentacene (Figure 2.1(c))). Due to their low solubility in solution as well as its poor environmental stability when in solid phase, their practical application is hindered [33–36] In order to solve the problems presented by this organic semiconductor, the Anthony group realized that these could be lessened by replacing the central ring of the pentacene's molecule [36]. This study compared the performance and stability of a solution-processed Organic Thin Film Transistor (OTFT) using 6,13-Bis(triisopropylsilylethynyl)pentacene (TIPS-Pentacene) - shown in Figure 2.1(b) - as active layer and vapor deposited Pentacene-OTFTs, and concluded that functional groups 6 and 13 of the TIPS-Pentacene prevent the oxidation of the molecule, making it more stable in atmospheric conditions, in terms of mobility. Thereby, the increase in the solubility of the molecule in organic solutions decreases most of dimerization reactions, and produces devices that exhibit a better carrier mobility. Another possible reason for the

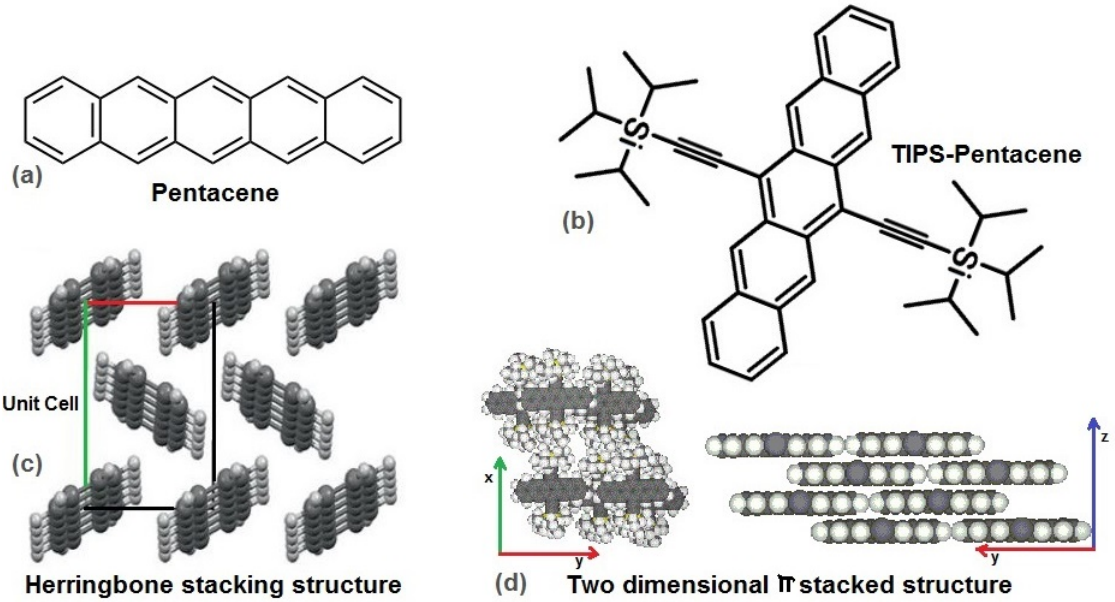

Figure 2.1: Molecular and stacking structure of pentacene (a and c) and of TIPS-Pentacene (b and d, respectively). This figure has adapted from [30, 31]

improvement stability of mobility, and also the I_{ON}/I_{OFF} ratio, is the 2-dimensional π-stacking (Figure 2.1(c)). This stacking herringbone is more compact for TIPS-Pentacene than for pentacene, as shown in a 2D structure (2.1(d)). This difference on crystal structure may allow moisture or oxygen to diffuse more easily in pentacene, resulting in poorer stability [35–37]. With the addition of TIPS groups onto pentacene the overlap of HOMO orbitals is not optimized, although the flatness of the crystal structure leads to better electrical properties. In this ordered arrangement, the functional groups force the crystal structure and the acene backbones to stack on top of one another [35]. As it is discussed in section 4.2.1, the molecular packing at the semiconductor-dielectric interface plays an important role on the field effect charge carrier mobility in OFETs. That is, it is desired to have long-range order and alignment of the semiconductor material close to the dielectric-interface. For planar devices such as OFETs, materials with two-dimensional π-stacking interactions are good candidates for active layer because they provide the best devices performance and the most uniform films. Thereby, we use TIPS-Pentacene as the organic semiconductor p-type, and it shows to be quite efficient for applications in printed electronics. TIPS-Pentacene thin film can be grown in the OFET channel by using inkjet printing as a consequence of the fusion of ejected droplets in the transistor structure. It is important to note that to produce thin films of TIPS-Pentacene the best solvent was tetralin, as will be seen later, in a concentration 19.4 mg/ml which resulted in a viscosity of 2.1 mPa.s, and for TIPS-Pentacene/anisole solution tested, the concentration used was 19,9 mg/ml which resulted in a viscosity of 1.4 mPa.s.

Chapter 3

Experimental

3.1 Devices Fabrication

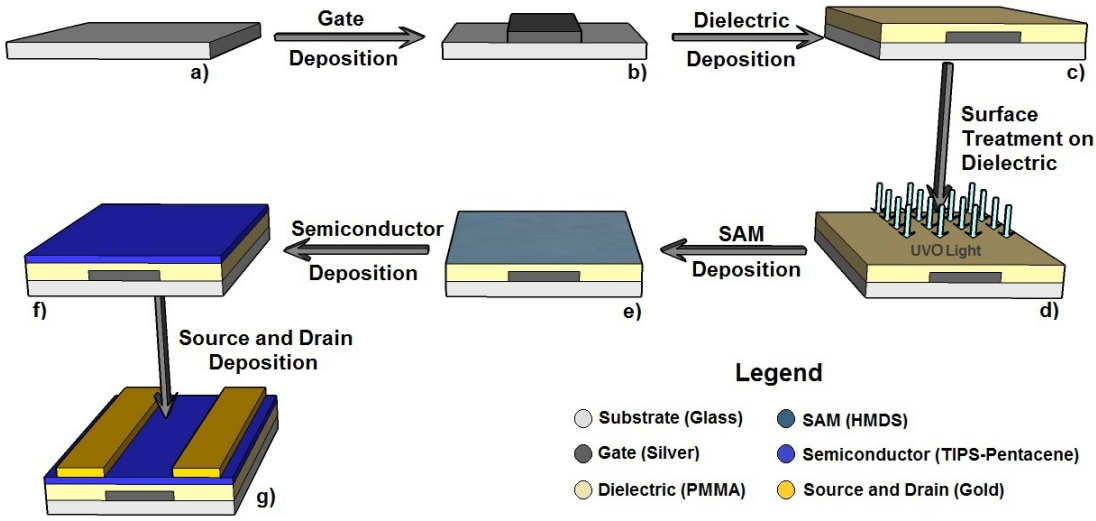

Figure 3.1: Schematic showing the process to obtain a OFET from a glass substrate previously clean (a), following to thermal evaporation of the gate (b), spin-coated dielectric film (c) leading to its surface treatment with UVO Radiation (d) and spontaneous evaporation of SAM (e), deposition of the TIPS-Pentacene by Inkjet Printer(f), and thermal evaporation of the source and drain contacts (g) respectively.

In the previous experimental preparation, essential to execute the experiments, several procedure steps were used to prepare the substrate and to built part of the transistors. These first stages of the research are worth mentioning in order to completely understand the development of the work described in this thesis. The device substrate, apart from providing mechanical support to the device, can affect the properties of the overlying deposited layers, and thereby plays a functional role in the final operation of the fabricated device. This section presents the procedure used, step by step, from the choice and the cleaning procedure of the substrate up to the deposition of the semiconductor layer by Inkjet Printing. Figure 3.1 shows (a) the a glass slide substrate that was cleaned by and ultrasonic bath with KOH and deionized water, then by a bath of boiling acetone and finally by an isopropanol bath. Next, in (b) the substrate has evaporated a 70 nm silver layer under vacuum to form the gate electrode, and in (c) it is depicted the dielectric layer (Poly(methyl methacrylate) (PMMA)) which was deposited by spin-coating technique from a solution having Butyl acrylate (nBA) as solvent, in a concentration of 70 mg/ml, inside a glovebox. Then, the dielectric was exposed to Ultraviolet Ozone (UVO) light (light-soaking) to remove eventual charged impurities[38] (d), and in an attempt to further improve the properties of the dielectric interface with the semiconductor, a self assembly monolayer of Hexamethyldisilazane (HMDS) was evaporated [38] onto the

PMMA surface (e). In (f) is shown the most important procedure of this work, which is the deposition of the organic semiconductor TIPS-Pentacene by inkjet printing. Finally, in (g) the manufacture of the transistor is completed by vacuum deposition of gold to form the source and the drain electrodes.

Gate and source/drain contacts were manufacturated using the shadow masks shown in Figure 3.1 thus enabling rapid production devices and the use of any desired architecture. The ratio W/L is 20 and in each sample are 9 transistors (T1 to T9) and one capacitor (C).

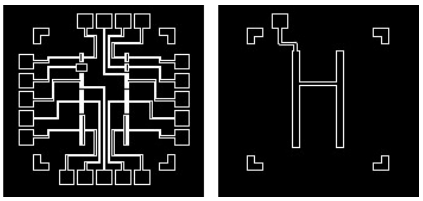

Figure 3.2: shadow masks used for evaporation of the contacts source/drain (left) and gate (right)

3.2 Inkjet

Printing Semiconductor Process

The Autodrop printer from the company Microdrop Technologies (see figure 3.3)[39] was used for this production step. The printing system is composed by a glass recipient (1) where ink is placed, and the dispensing system (2) with an orifice diameter of 70 µm. To print TIPS-Pentacene through this equipment was essential to prepare a low viscosity solution and capable of forming a continuous film (can sen on the section 4.3.2 the lines printed by the Microdrop).Furthermore, the solution must be filtered with a 45 µm filter to not clog the capillary.

To begin printing the following steps were necessary: (i) fill the print head with the solution, (ii) adjust dispensing parameters to trigger the drop formation (Figure3.3 c)), (iii) adjust grid parameters for attaching the drops and then to form a continuous film, and (iv) set the speed for the x-axis and the y-axis with sliding tools during the "In Flight Dosing" (see table 4.1). Once the printing optimization parameters were established the TIPS Pentacene were deposited between the source and the drain in a way to avoid solution waste. The substrate was heated to a temperature of 36 and 46°C so as to control the rate of solvent evaporation.

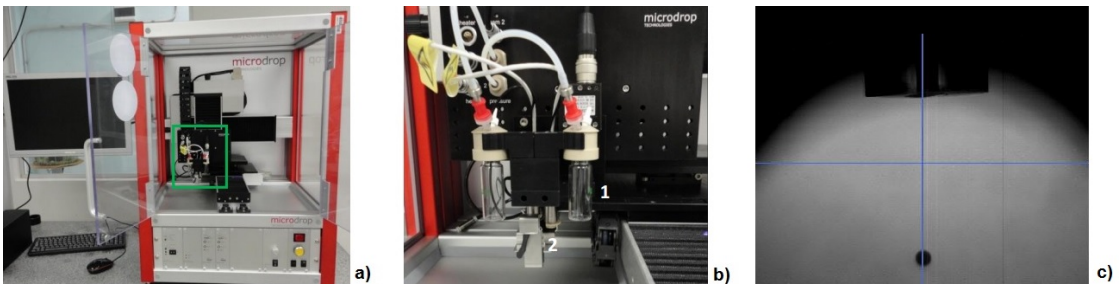

Figure 3.3: Printer Autodrop. Printer Overview (a) and expansion of the area highlighted in green showing printing system (b) Drop Formation of the TIPS Pentacene (c)

Chapter 4

Analyse of the Dielectric and Active Layer

4.1 Device's Architecture

As previously mentioned, the purpose of this study is to optimize the semiconductor active layer printing with the objective to improve the technology of printed OFETs. Previous studies of various aspects are then crucial steps to achieve this goal with success. The first definition we need to establish is the type of architecture of our transistor. It is well reported in the literature that Bottom Gate/Top Contact (BG/TC) structure exhibits relatively high field effect mobility for certain p-type small molecules, as TIPS-Pentacene [40–42].The reason for the good electric performance is often explained by the reduced value of the contact resistance on the interface electrodes/OSC, which would be caused by an increase in the area for charge injection [43]. In addition, it has been observed that in case of bottom contact, the semiconductor film patterned around source and drain leads to contacts that present a poor morphology. [44].

4.2 Dielectric Layer

The choice of dielectric is also another important step, whose dielectric properties and processing strongly influence to the final characteristics of the printed device. The function of this layer is not only to electrically isolate the gate electrode from the source and drain electrodes, but mainly from the semiconductor channel. An ideal dielectric layer forms a capacitor where one electrode is the gate, and its function is to establish an electric field in the dielectric / semiconductor interface . The role of this electric field is to control the current along the channel, both in the linear and in the saturation regimes. In this sense, not only the bulk properties of the dielectric film are essential for the good performance of the BG/TC, but also the roughness and the superficial energy of the dielectric surface are extremely relevant to avoid any negative effect on the charge carrier transport along the semiconductor layer. It has already been shown that the dielectric interface plays a non negligible role in the molecular organization of the OSC film, which is formed onto the dielectric layer, mainly in the molecular packing and in the crystallization process [44]. Today there is a great effort of research in order to find an organic dielectric material that has high electrical resistivity, high-value dielectric constant and that is chemically orthogonal with the best solvents used for conjugated molecules. Despite the advantageous properties of Poly(vinylpyrrolidinone) (PVP), the adherence of the semiconductor layer on PVP was very poor, which results in a non uniform and non-crystalline deposited film. After testing other dielectrics, we decided to use the classic PMMA. This is because, after studying different surface treatment processes and tests of wettability, PMMA showed up as the most suitable, although their dielectric constant is still low for a good performance as dielectric layer of an OFET. However, we believe that it is worth insisting on PVP processing study as an alternative to PMMA. Perfilometry

measurements carried out with several PMMA layers showed that it exhibits an average thickness of 540 nm.

4.2.1 Dielectric/semiconductor Interface Treatment

As mentioned throughout the text, the interface semiconductor/dielectric plays a crucial role in the performance of an OFET, and this subject has been extensively investigated in the last years due to the direct impact caused on the semiconductor morphology and/or on the generation of trap-defect at the interface causing the decrease of the charge carrier mobility. Two aspects are determinant in the choice of the dielectric: their structural and dielectric properties and its chemical compatibility with adequate solvents. Once deposited the dielectric film, i. e. overcame the difficulties of the film deposition, the next step is to eliminate the deleterious effects of electrostatic origin, which act against the transport properties of the active layer. Thereby, in order to improve the characteristics of the PMMA/TIPS-Pentacene interface we carried out the following procedure: i) the PMMA was treated with UVO radiation to increase reactive groups present on its surface; ii) a self-assembled monolayer of HMDS was evaporated on the UVO-treated PMMA surface. This treatment improved considerably the roughness of the PMMA surface and the wettability of the semiconductor over the dielectric layer, having as a consequence improvement of threshold voltage and the charge carrier mobility. It was also observed by other authors that the work function of source and drain contacts was also positively affected [45].

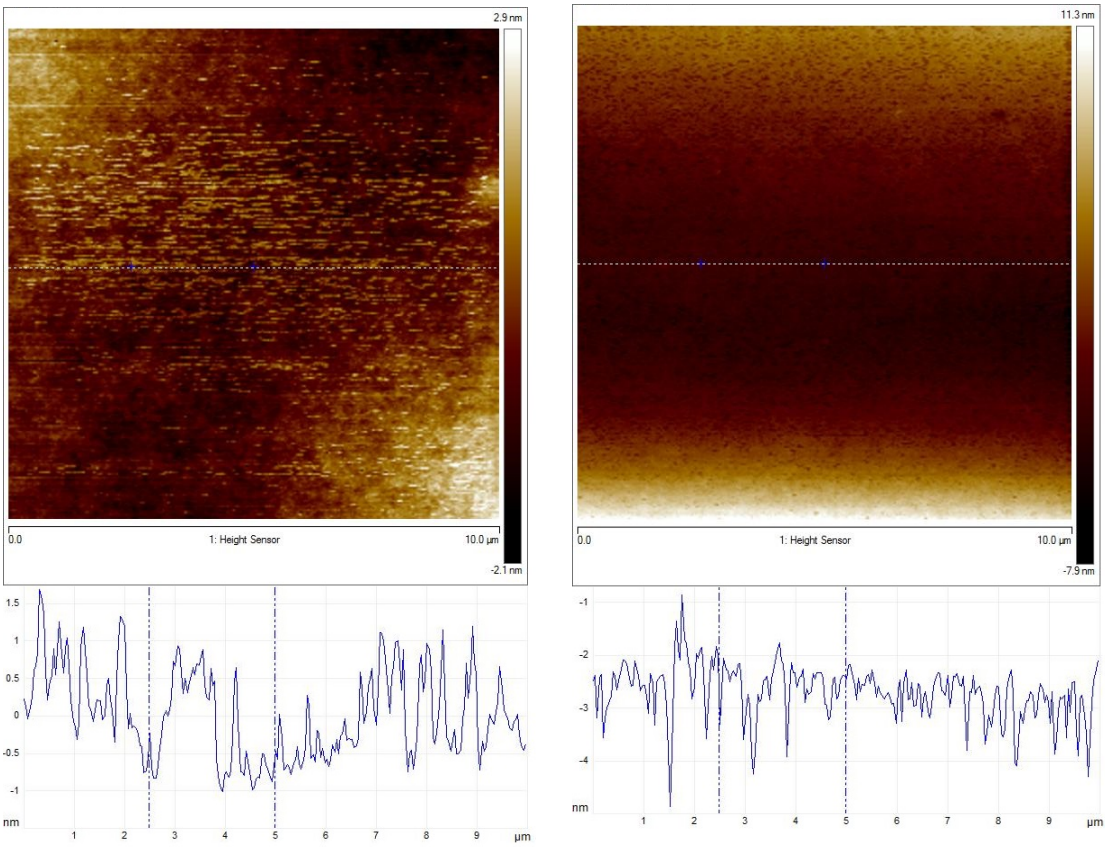

(a) (b)

Figure 4.1: RMS roughness of PMMA (a) without treatment; (b) with 7s UVO treatment

Figure 4.1 shows the AFM images of PMMA without (a) and with the UV-treatment (b), which changed the root mean square (RMS) of the roughness. The RMS value increased from approximately 0.75 nm (wihtout treatment) to 3.2 nm (with treatment). Despite the increase in the roughness, we observed from Figure 4.1 that the UV-treatment induced an increase in the film's uniformity. We also studied the effect of the HMDS monolayer on the cristallization of the TIPS pentacene film, as shown in Figure 4.2. From the analysis of the reflection due to the (001) orientation obtained from X-Ray Diffraction spectra (XRD) we can infer that this treatment enhanced substantially the crystallinity degree of the deposited semiconductor films, irrespective whether the solvent for the TIPS-Pentacene was Anaysol or Tetralin.

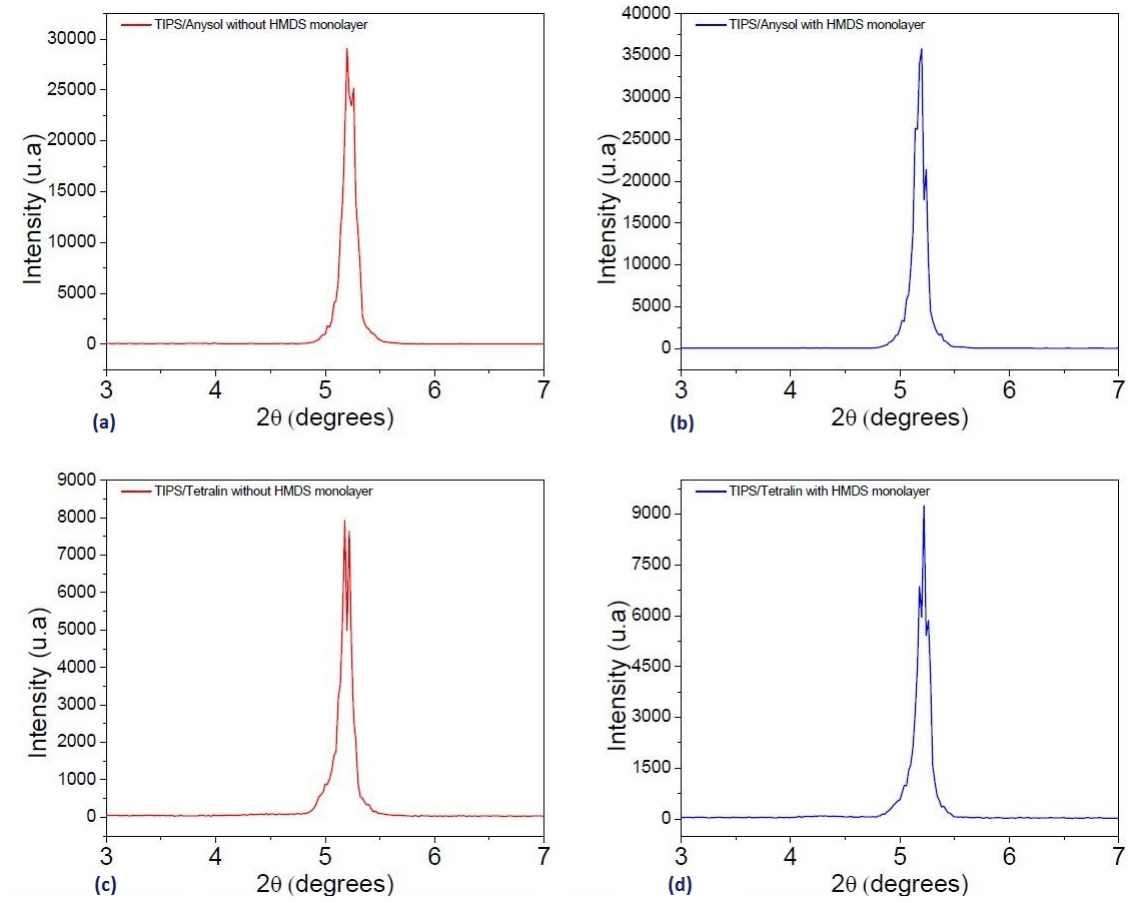

Figure 4.2: The results of XRD spectroscopy of different TIPS-Pentacene solvents with (b and d) and whithout (a and c) HMDS monolayer

4.3 Semiconductor Layer

First we invested in manufacturing a transistor p-type, which we use as organic semiconductor TIPS-pentacene molecule because it exhibits good electronic properties, and also superior solubility and stability when compared with other conjugated organic molecules.

4.3.1 Semiconductor Solvent

After a previous choice with the help of the literature and taking into account the solvent's orthogonality, we choose two solvents for TIPS-pentacene. The first solvent used was 1,2,3,4-tetrahydronaphthalene (tetralin), which is a hydrocarbon molecule whose chemical structure is shown in Figure 4.3 a), having a formula $C_{10}H_{12}$. The second was methoxybenzene, whose formula is $CH_3OC_6H_5$, and the structure is shown in Figure 4.3 b).

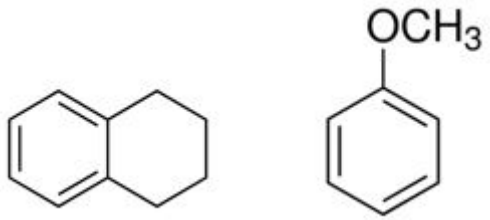

Figure 4.3: Structural formula of: (a) tetralin, and (b) anisole

In theory these two solvents fulfill the basic requirements to prepare a printable ink-TIPS Pentacene, i. e. high solubility, provided by the aromatic structure, as well as adequate boiling point and viscosity [40, 42, 46, 47]. Aromatic solvents are suitable for this application because their molecules solvate the π-electron of conjugated molecule, improving the π-stacking, and hence the electrical conductivity of the formed film.

4.3.2 Printed Parameters for Semiconductor Layer

Since the Microdrop printer can control a multitude of printing parameters, we performed a detailed study to determine the best parameters for each TIPS Pentacene-solution, i. e. different solutions varying the solvent (tetralin or anisole) and the concentration. The obtained results are shown in table 4.1.

Table 4.1: Parameters used to optimize the printing TIPS-Pentacene/Tetralin and TIPS-Pentacene/Anisole

	Parameters	**Tetralin Solvent**	**Anisole Solvent**
Drop Formation	Voltage	75-80 V	70-75 V
	Pulse Width	30-35 μs	30-35 μs
	Frequency	500Hz	500Hz
	Pressure	-15mbar	-15mbar
Grid Parameters	Grid Pattern	Pattern 2	Pattern 2
	Grid Distance	330 μm	250 μm
"In Flight Dosing"	Speed for the axes	2 mm/s	1 mm/s

It should be noted that the Grid Distance parameter, for example, for obtaining the best results in printing multiple lines, exhibited different values of spacing drops for tetralin and anisole. Figure 4.4 shows images for printed TIPS-Pentacene/Anisole lines obtained using an optical microscope Olympus BX 41. From the images one can observe that the line is formed when the spacing drop is below 350 μm, and that separated drops are printed for spacing of drops of 400 µm and above. More specifically, for spacing drops below and equal to 290 μm we can ensure a good line formation, i. e. lines having a good parallelism between the lateral edges. Above 290 µm the printed lines exhibit a periodic sinusoidal profile. Similar results were obtained for solutions of TIPS-Pentacene/Tetralin, in which the limit between line and separated drops formation was 330 μm.

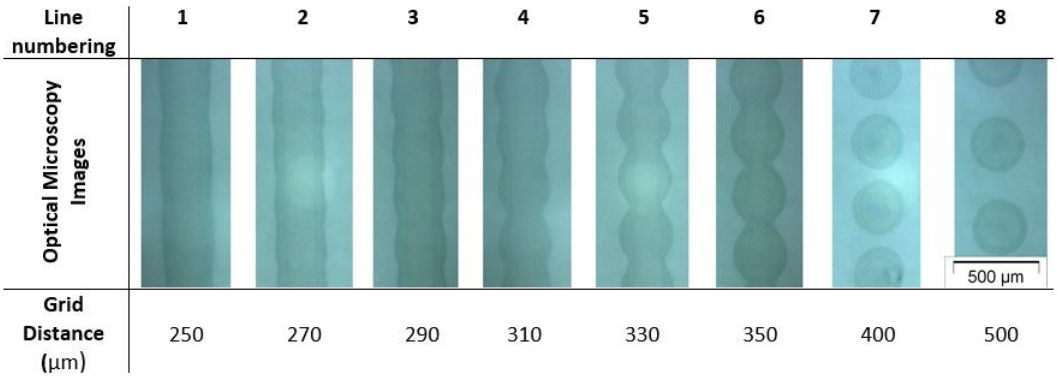

Figure 4.4: Printed TIPS-Pentacene/Anisole lines with different values of spacing drops

As already mentioned above, an undesirable effect difficult to be avoided during the drop printing is the formation of the Coffee Ring effect, as shown in Figure 4.5. This effect is caused during the solvent evaporation, which is more intense at the drop's edges. This evaporation asymmetry stimulates the flows of mass from the drop center to the edge, resulting in a higher accumulation of molecules in the edges in comparison to the center of the drop. According to Tekin et al. [48] a way to alleviate this problem, and to get more homogeneous films is to use a mixture of solvents having high and low boiling points. In such mixture, the solvent with a lower boiling point would evaporate more slowly, and then gradually decreasing the flows of mass. A suggestion for the continuity of this work is to find a good solvent for the TIPS-Pentacene that has a lower boiling point in comparison to tetralin (207°C) or anisole (154°C).

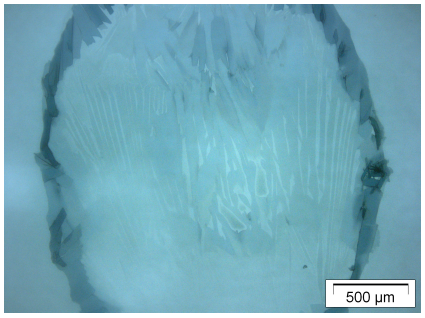

Figure 4.5: Coffee Ring Effect

Once the parameters that optimize the TIPS-pentacene printing were defined, and from the analysis of the best printed lines, both in using Tetralin or Anisole as solvent (Figure 4.4), we reached some important remarks. First, the TIPS-Pentacene printed line (in anisole) presented na undesirable result arising from the Coffe Ring effect (Figure 4.6(a)). Second, crystalline structures were formed in printed lines (in tetralin), which is crucial for a good performance of the charge transport along the semiconductor channel, as already described in Section 1.5. This crystallinity is clearly shown in Figure 4.6(b), which also indicates that the long crystallites were arranged in an organized manner forming a herringbone structure. The conclusion obtained from these two points is that the printed line of TIPS-pentacene dissolved in tetralin, despite its highest boiling point, is more efficient to built a semiconductor channel for an OFET. This can be explained by the fact that the substrate was heated during the printing procedure.

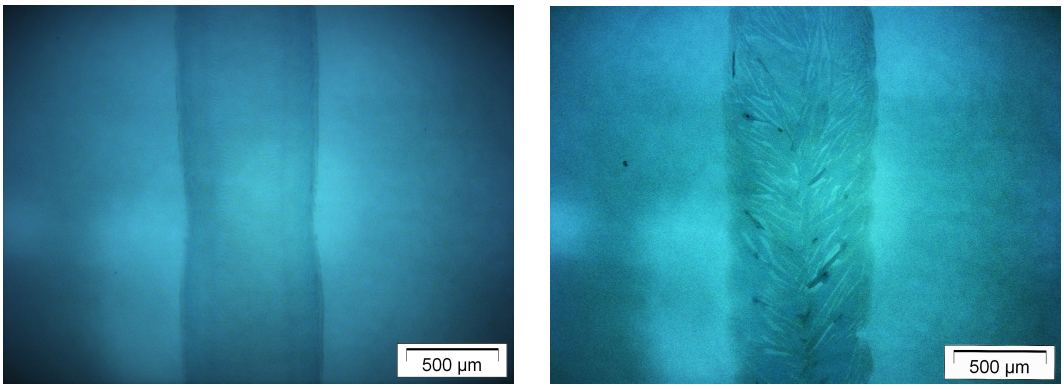

(a) (b)

Figure 4.6: Crystalline structures formed in printed (a) TIPS-Pentacene/Anisole lines to 250 μm spacing drops and (b) TIPS-Pentacene/Tetralin lines to 330 μm spacing drops

The organization of the crystals shown in Figure 4.6 raised interest,thus a study to further characterize these formations via X Ray Diffraction (XRD) and Scanning Electron Microscope (SEM) was conducted.

4.4 Structure and Morphology of the Printed Layers

4.4.1 Images of Scanning Electron Microscope

SEM images shown in Figure 4.7 reinforce that the TIPS-Pentacene dissolved in tetralin (Figure 4.7(b)) results in higher crystalline films when compared to the solution of anisole (Figure 4.7(a)). These images are captured from films formed by drop-casting technique, in which TIPS-pentacene dissolved in tretralin shows long and oriented crystallites with circa of 20 μm of length in drop-casting films. In Figure 4.8, similar SEM images of inkjet printed TIPS-pentacene films are shown; again with anisole and tetralin. From these last images we can observe that there is failure in the formation of TIPS-pentacene film when dissolved in anisole, i.e. the printed lines do not merge, avoiding the formation of uniform films. This undesirable result most probably is a consequence of the Coffee Ring effect shown in Figure 4.5. On the other hand, the printed films formed from pentacene-tetralin solution showed good uniformity and a high degree of crystallinity in a well defined orientation (Figure 4.8(b)).

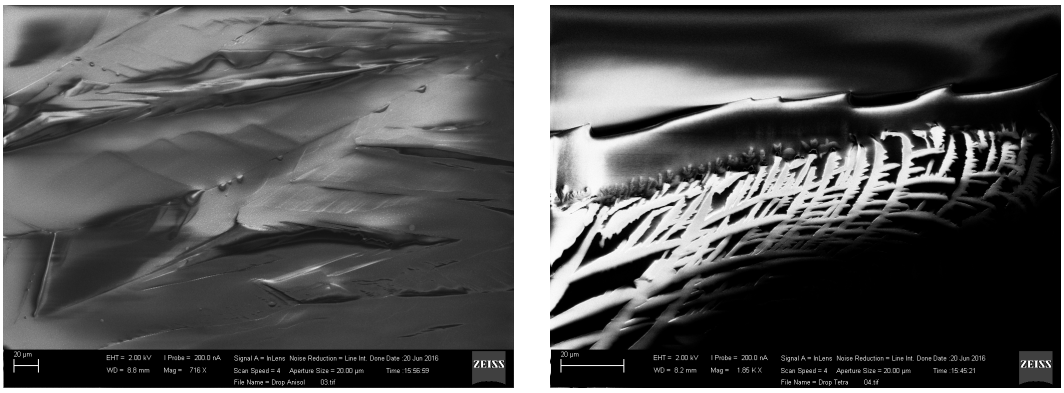

(a) of TIPS-Pentacene/Anisole (b) of TIPS-Pentacene/Tetralin

Figure 4.7: Analyzed SEM image and crystalization of an thin films formed by drop casting technique

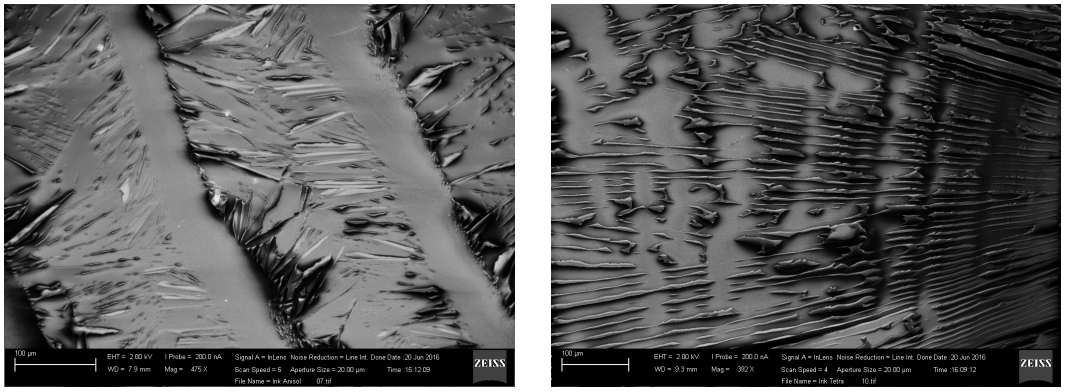

(a) of TIPS-Pentacene/Anisole (b) of TIPS-Pentacene/Tetralin

Figure 4.8: Analyzed SEM image and crystalization of an thin films formed by inkjet printing

4.4.2 Wide-Angle X-ray Diffraction

Wide-Angle X-ray Diffraction (WAXD) patterns of TIPS-pentacene films were obtained by a Rigaku Rotaflex RU 200B instrument (Cu Kα radiation, $\lambda = 1.5418\,\text{Å}$), operating with 40 kV and 80 mA. The films were deposited onto a PMMA previously functionalized with HMDS, supported by a glass substrate. Figures 4.9(a) and 4.9(b) show, respectively, the X-ray diffraction pattern of the nude substrate (glass) and that of the substrate coated with a thin film of functionalized PMMA. The amorphous characteristic is evidenced by the broad peak centered 2θ equal to 24°. When a printed thin film of TIPS-Pentacene is deposited on the top of the HMDS-PMMA (that whose WAXD is shown in Figure 4.9(b)), the new recorded X-ray diffractogram is completely different, as shown in Figure 4.10(a). This diffractogram confirms the high crystallinity degree of the printed TIPS-pentacene from a tetralin solution. Just for comparison, we present a diffraction pattern obtained from a thick film of TIPS-Pentacene (Figure 4.10(b)), also from a tetralin solution, which shows the same diffraction peaks displayed in Figure 4.10(a).

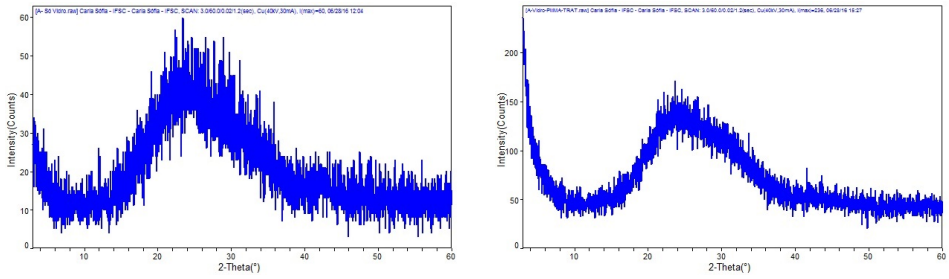

(a) (b)

Figure 4.9: WAXD obtained from: a) nude glass substrate; and b) the same substrate coated with PMMA functionalized with HMDS.

Anthony et al. [49] Single-crystal TIPS-Pentacene has a triclinic structure with unit cell parameters $a = 7.5650\,\text{Å}$, $b = 7.7500\,\text{Å}$, $c = 16.835\,\text{Å}$, $\alpha = 89.15°$, $\beta = 92.713°$, and $\gamma = 83.63°$. The peak observed at about 5.2° corresponds to intermolecular spacing of 16.8 Å, indicating preferential orientation of (001)-axis normal to the surface. The peaks that appeared at 10.4° and 15.8° were identified with the (002) and (003) orientation, respectively.

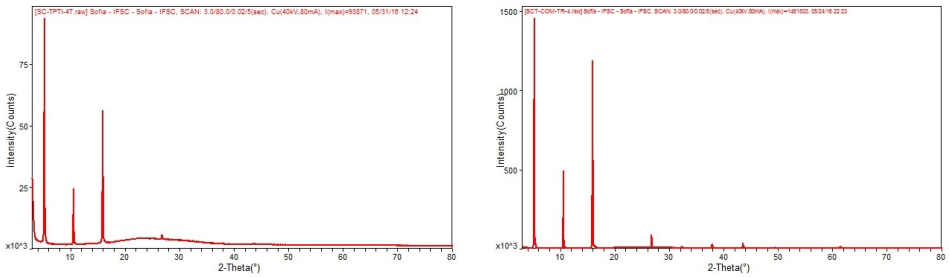

(a) (b)

Figure 4.10: WADX obtained from TIPS-pentacene film deposited by: a)inkjet printing on the substrate coated with PMMA functionalized with HMDS; b)drop casting

Chapter 5

OFETs and Inverter

Since the purpose of this work is to take the first steps for printing logic circuits made with organic semiconductors, the first and important step is to master the printing of the active layer of an organic transistor. This chapter shows the results obtained with a p-type OFET and the application in a p-MOS inverter. In the last section we present the first results with a n-OFET. The continuity of research in these two transistors, n and p types, will open numerous possibilities in the area of printed organic circuits, especially from the printing of an organic complementary circuit.

5.0.1 OFETs: Drain current (I_D) versus source-drain voltage (V_D)

The quality of inkjet printed TIPS-Pentacene films as active layer in the p-OFET channel is directly affected by the solvent used in the electronic ink, as shown in Figure 5.1. Figure 5.1(a) shows that the drain current (I_D) versus source-drain voltage (V_D), having different gate voltages, when anisole was used as solvent presented a significant leakage current. On the other hand, I_D x V_D responses obtained with similar transistor now using TIPS-Pentacene dissolved in tetralin, not only eliminated the undesirable leakage current, but also exhibited higher drain current (almost one order of magnitude higher), as shown in Figure 5.1(b). This improvement is a direct consequence of the better printed film as discussed in the previous section when tetralin is used as the solvent. This solution produced more uniform and crystalline films. It is important to remark that the relatively high values for the operation voltage are due to the low dielectric constant of the PMMA. In this research area the search for better organic materials to be used as a dielectric layer for OFETs is the challenge to be overcome currently.

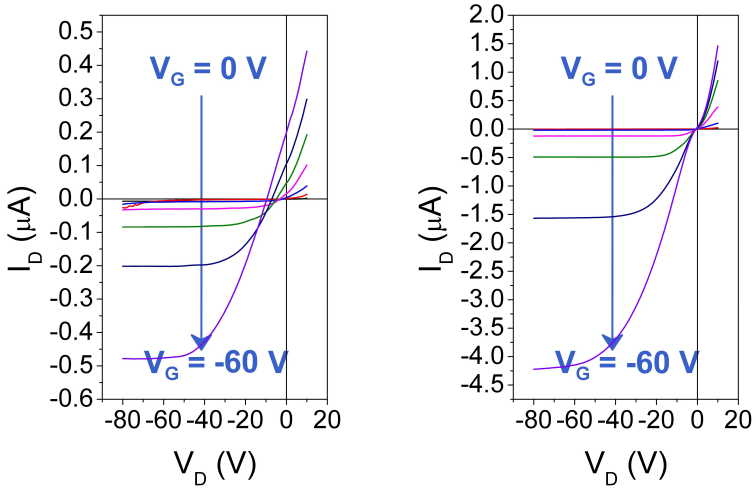

(a) (b)

Figure 5.1: Drain current vs Drain-source voltage of p-OFETs: a) TIPS-pentacene dissolved in Anisole; b) TIPS-pentacene dissolved in Tetraline

5.1 p-OFETs-tetralin

Since tetralin showed to be a superior solvent for TIPS-pentacene, we seek to optimize the performance of the printed transistors by varying the rate of solvent evaporation. To do this, the substrate was heated during the deposition of TIPS-pentacene into transistor channel. This was possible due to heating feature available in the Microdrop printer. Figure 5.2 shows experiments carried out with a transistor (A1) whose substrate was heated at 36°C. In addition to the $I_D - V_D$ curve (5.2a), experimental results of $I_D - V_G$ transfer characteristic (5.2b), and the curves $(I_D.L/W)^2$ x V_G and $Log(I_D.L/W)$ x V_G (5.2c), were also analyzed. From these experimental curves it was possible, as shown in the Appendix, to obtain values for the charge carrier mobility (μ_{OFET}), the I_{ON}/I_{OFF} ratio, and the value for the subthreshold swing (S = dV_G/d(logI_D)).

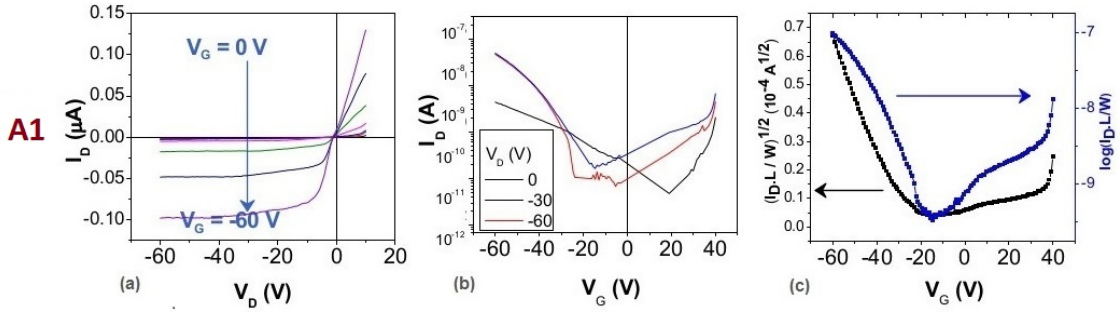

Figure 5.2: Characteristic curves of a p-OFET printed at 36°C: (a) $I_D - V_D$ curve; (b) $I_D - V_G$ transfer characteristic; and (c) $(I_D.L/W)^2$ x V_G and $Log(I_D.L/W)$ x V_G curves.

Table 5.1 exhibits the characteristics values for three similar transistors, all of them heated at 36°C during the printing procedure, added by the calculated values for the capacitance C of the dielectric layer and the threshold voltage V_{Th}. From such results we can infer that we need to optimize the fabrication procedure to improve the transistor's performance and the reproducibility.

Table 5.1: Parameters obtained for p-OFETs (TIPS-Pentacene with tetralin) heated at 36°C during the printing procedure.

Transistors	**C** F/cm^2	V_{Th} V	μ_{OFET} cm^2/V.s	I_{ON}/I_{OFF}	**S** V/dec.
A1	3.7E-9	-26.58	0.00209	134	27.03
A2	3.8E-9	-11.51	0.00727	434	13.28
A3	3.3E-9	-14.68	0.03005	376	12.88

Similar procedure was carried out with transistor in which the substrate was heated at 46°C. The results are shown in Fig5.3. The parameters are displayed at Table 5.2.

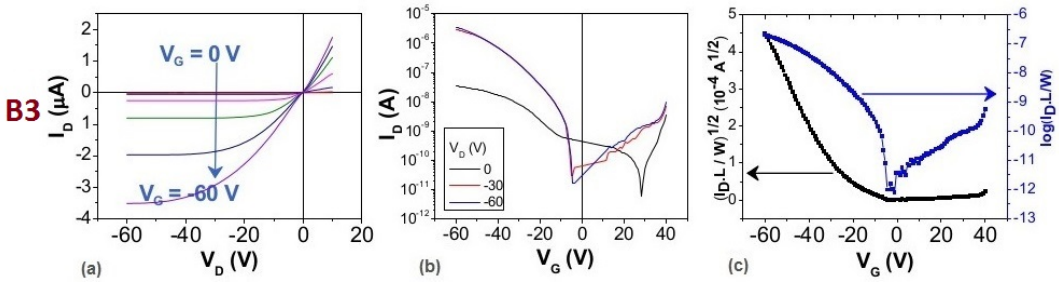

Figure 5.3: Characteristic curves of a p-OFET printed at 46°C: (a) $I_D - V_D$ curve; (b) $I_D - V_G$ transfer characteristic; and (c) $(I_D.L/W)^2$ x V_G and $Log(I_D.L/W)$ x V_G curves.

Table 5.2: Parameters obtained for p-OFETs (TIPS-Pentacene with tetralin) heated at 46°C during the printing procedure.

Transistors	**C** F/cm^2	V_{Th} V	μ_{OFET} cm^2/V.s	I_{ON}/I_{OFF}	**S** V/dec.
B1	9.77E-10	-14.89	0.17066	10110	4.98
B2	9.77E-10	-20.44	0.30274	7672	6.81
B3	1.55E-8	-22.43	0.01823	52950	1.68

We observed that the capacitance did not change significantly from one transistor to another, at least for those heated at 36°C. For those heated at 46°C, only the transistor B3 showed a different value for the capacitance. On the other hand, the threshold voltage was more uniform for the transistors heated at 46°C, and also they presented higher values for the mobility, I_{ON}/I_{OFF} ratio and subthreshold swing S.

5.2 Inverter Characterization

The main function of an inverter circuit is to invert the applied input signal. A simple inverter can be constructed by using a single p-OFET coupled with a resistor, as depicted in Figure 5.4, in which the load resistance is in series with the drain electrode and the source is grounded. The opposite side of the resistor is connected to the to the supply voltage (V_{DD}), and when $V_{in} = 0$ (logic 0), the transistor is off and no current flows through the resistor, and $V_{out} \equiv 1$. However, for $V_{in} = V_{DD}$ (logic 1) , it results in $V_{out} \equiv 0$ (Table 5.3).

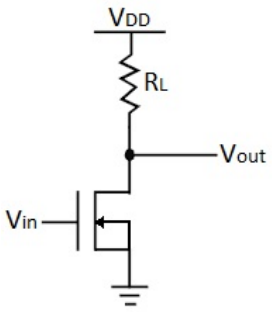

Figure 5.4: PMOS inverter with a resistor load

Table 5.3: Truth Table

V_{in}	V_{out}
0	1
1	0

For our experiment we used a resistor-transistor inverter circuit first with a V_{DD} = 60 V, and varied the R_L from 50 to 300 MΩ, sweeping the V_{in} from -60 V to zero. The result is shown in Figure 5.5a. Figure 5.5b show similar V_{out} X V_{in} curve for a R_L = 300 MΩ, for different values of V_{DD} (from 20 to 60 V); amd Figure 5.5c shows the gain curve of this circuit for V_{DD} = 60 V and R_L = 300 MΩ.

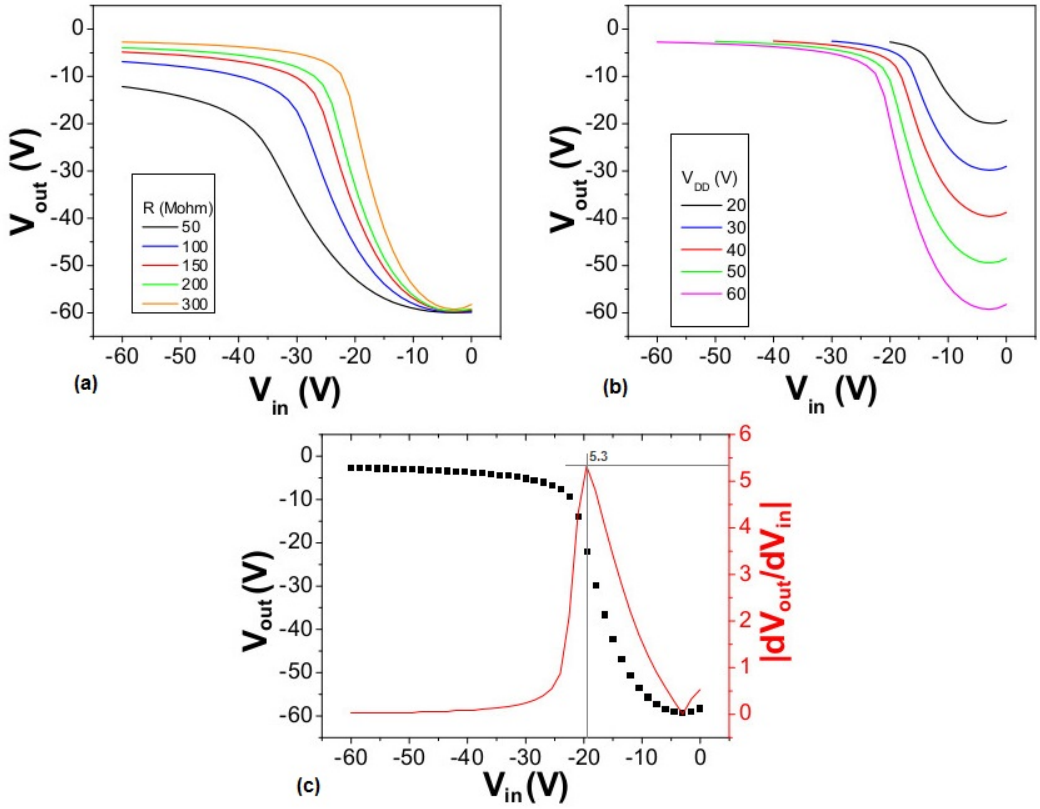

Figure 5.5: Curves of voltage transfer characteristics of the digital inverter. (a) Effect of resistance for $V_{DD} = 60V$; (b) Effect of variation of tension for R=300MΩ; (c) VTC curve with drive voltage gain for $V_{DD} = 60V$ and R=300MΩ

5.3 n-OFET

Here we present preliminary results on n-OFET manufacturing by inkjet printing. The structure chosen for the n-OFET was also BG / TC, and the semiconductor was the conjugated molecule P(NDI2OD-T2) (ActiveInk™N2200), shown in Figure 5.6 This molecule was dissolved in p-xylene in a concentration of 3 mg/ml, and after printing it in the channel, the transistor was annealed at 200°C during 30 minutes.

Figure 5.7 displays results of the same experiments as carried out with p-OFETs, i. e. the I_D-V_D curve (5.7a), the ID-VG transfer characteristic (5.7b), and the curves $(I_D.L/W)^2$

x V_G and $Log(I_D.L/W)$ x V_G (5.7c).

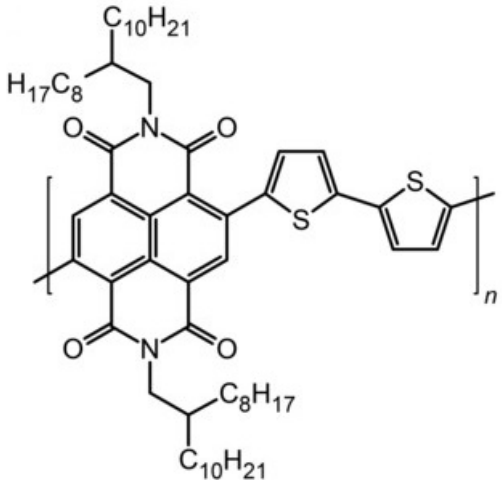

Figure 5.6: Molecular structure of P(NDI2OD-T2)

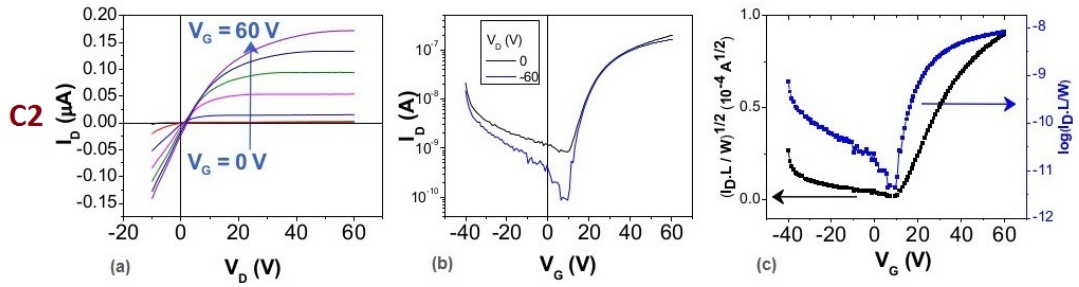

Figure 5.7: Characteristic curves of a n-OFET: (a) $I_D - V_D$ curve; (b) $I_D - V_G$ transfer characteristic; and (c) $(I_D.L/W)^2$ x V_G and $Log(I_D.L/W)$ x V_G curves.)

Table 5.4: Parameters obtained for n-OFETs

Transistors	**C** F/cm^2	V_{Th} V	μ_{OFET} cm^2/V.s	I_{ON}/I_{OFF}	**S** V/dec.
C1	8.59E-9	10.13	1.35E-4	21	10.99
C2	8.59E-9	9.67	0.00138	474	3.28
C3	8.59E-9	-21.50	3.26E-4	0.17	56.31

Despite the Field-effect operation shown by the family of curves displayed in Figure 5.7a, the parameters extracted from three first fabricated transistors are still very poor and need improvements. However, being these results the first, they are promising. With the improvement of the performance of n and p OFETs, it will be possible in a near future to build printed complementary organic circuits.

Chapter 6

Conclusions and Final Remarks

Printed electronics is a new branch inside processing and novel materials for electronics. This area is growing fast and is revealing a promising and huge market in the near future. Several printing techniques for electronics have been developed in the last years, as offset lithography, flexography, rotogravure, serigraphy, and Inkjet. In this scenario, this thesis proposes to use inkjet printing technique to deposit organic films as the semiconductor layer in the channel of OFETs. First we use the TIPS-Pentacene, which is an p-type organic semiconductor, to conduct a study of the best solvent for having the adequate fluidic parameters to achieve good printed thin films in the channel. We identified the tetralin as an organic solvent that fits well the required printing conditions. We used an Autrodrop model of Microdrop company as the printer, which uses a Drop-on-Demand system via a piezoelectric ejector. The organic film was printed over a thin film of PMMA, which played the role of the dielectric layer in the transistor. In order to optimize the printing process of TIPS-Pentacene thin-films applied on OFET Technology, an extensive study boarding several parameters was performed:

(i) BG/TC architecture was chosen due to the high field effect mobility present by the devices. This architecture presents a low contact area for charge injection, which leads to a reduced contact resistance. The combination of these two parameters originated devices with a good electrical performance;

(ii) The choice of polymeric material used as insulator between the gate electrode and the semiconductor channel was limited to a few materials. PMMA was choised due to it excellent properties as electrical insulator. However, PMMA has a low dielectric constant. Today, new polymers with higher values of dielectric constant are emerging in the market, which should improve the performance of organic transistors, especially in lowering its operating voltage;

(iii) Since the morphology of the dielectric/semiconductor interface is a crucial parameter for the device's performance, a surface treatment consisting of UV-Ozone radiation followed by a deposition of a HMDS monolayer was applied to this interface. AFM results show that the roughness's RMS suffered an increase after the applied treatment (0.75 to 3.2 nm), consequence of the added functional groups that result from the UVO treatment. As for the XRD spectra (with and without HMDS), we can conclude that the crystallinity of TIPS-Pentacene is increased when HMDS is added to the interface;

(iv) The TIPS-Pentacene film's morphology has a strong dependence on the chosen solvent. In order to achieve the most suitable morphology, a detailed study to the TIPS-Pentacene was carried out using microscopy techniques and WAXD. Besides providing a better structural morphology with desired electrical properties, the used solvent needs to be an orthogonal solvent for the dielectric layer (PMMA). We found that the solvent tetralin provided well organized TIPS-Pentacene films with a high crystallinity degree,

making this the most suitable solvent;

(v) The transistors were fabricated with two different substrate temperatures (36 and 46°C) and further characterize be means of Drain current vs Drain-source voltage, I_D V_G transfer characteristic,$(I_D.L/W)^2$ x V_G and $Log(I_D.L/W)$ x V_G curves. The transistors presented higher values of mobility and I_{ON}/I_{OFF} ratio at 46°C than at 36°C. The obtained mobility and values I_{ON}/I_{OFF} ratio are in concordance with the ones described in the literature. Interestingly, the subthreshold voltage (S) suffered a significant increase (-$10^{-}3$ to 1 V/dec), which is not good for the performance of the transistors, since higher values of S result in higher gate voltages required to improve the drain current in one decade.

Using the most suitable parameters determined in the previous studies, we were able to fabricate a p-OFET in an resistor-transistor inverter with a gain of 5.3.

The literature is abundant in organic semiconductor of p-type, but only recently good and processable n-type organic molecules have been synthesized. What we intend for the continuity of this work is to build p-OFETs and n-OFETS with similar characteristics, so to pave the way for the fabrication of a complementary organic circuits, a CMOS type. With this in mind, we obtained the first results of a printed n-OFETs using the P(NDI2OD-T2) molecule as semiconductor. We succedded in keeping the same geometric architecture used for the p-OFET (BG/TC), since we can use the same mask and the same substrate for printing both the p and n OFET side by side.

These preliminary results showed that we are in the right direction, and for future developments the aim is to dominate the fabrication of a printed n-OFET that matches the characteristics of a p-OFET, so that the fabrication of a complementary organic circuit can be achieved.

Bibliography

[1] J. R. Sheats, D. Biesty, J. Noel, and G. N. Taylor. "Printing technology for ubiquitous electronics". In: *Circuit World* 36.2 (2010), pp. 40–47. ISSN: 0305-6120. DOI: 10.1108/03056121011041690.

[2] A. Loi, L. Basiric??, P. Cosseddu, S. Lai, M. Barbaro, A. Bonfiglio, P. Maiolino, E. Baglini, S. Denei, F. Mastrogiovanni, and G. Cannata. "Organic bendable and stretchable field effect devices for sensing applications". In: *IEEE Sensors Journal* 13.12 (2013), pp. 4764–4772. ISSN: 1530437X. DOI: 10.1109/JSEN.2013.2273173.

[3] J. Fernandez-Salmeron, A. Rivadeneyra, M. A. C. Rodriguez, L. F. Capitan-Vallvey, and A. J. Palma. "HF RFID Tag as Humidity Sensor: Two Different Approaches". In: *IEEE Sensors Journal* 15.10 (2015), pp. 5726–5733. ISSN: 1530-437X. DOI: 10.1109/JSEN.2015.2447031.

[4] R. S. Deol, H. W. Choi, M. Singh, and G. E. Jabbour. "Printable displays and light sources for sensor applications: A review". In: *IEEE Sensors Journal* 15.6 (2015), pp. 3186–3195. ISSN: 1530437X. DOI: 10.1109/JSEN.2014.2378144.

[5] K. J. Baeg, D. Khim, J. H. Kim, M. Kang, I. K. You, D. Y. Kim, and Y. Y. Noh. "Improved performance uniformity of inkjet printed n-channel organic field-effect transistors and complementary inverters". In: *Organic Electronics: physics, materials, applications* 12.4 (2011), pp. 634–640. ISSN: 15661199. DOI: 10.1016/j.orgel.2011.01.016.

[6] S. Lim, B. Kang, D. Kwak, W. H. Lee, J. A. Lim, and K. Cho. "Inkjet-printed reduced graphene oxide/poly(vinyl alcohol) composite electrodes for flexible transparent organic field-effect transistors". In: *Journal of Physical Chemistry C* 116.13 (2012), pp. 7520–7525. ISSN: 19327447. DOI: 10.1021/jp203441e.

[7] A. Tsumura, H. Koezuka, and T. Ando. "Macromolecular electronic device: Field-effect transistor with a polythiophene thin film". In: *Applied Physics Letters* 49.18 (1986), pp. 1210–1212. ISSN: 00036951. DOI: 10.1063/1.97417.

[8] G. Horowitz, X. Peng, D. Fichou, and F. Garnier. "The oligothiophene-based field-effect transistor: How it works and how to improve it". In: *Journal of Applied Physics* 67.1 (1990), pp. 528–532. ISSN: 00218979. DOI: 10.1063/1.345238.

[9] M. Kitzler, X. Xie, S. Roither, A. Scrinzi, and A. Baltuska. "Angular encoding in attosecond recollision". In: *New Journal of Physics* 10 (2008), pp. 0–13. ISSN: 13672630. DOI: 10.1088/1367-2630/10/2/025029.

[10] G Horowitz. "Organic field-effect transistors". In: *Advanced Materials* 10.5 (1998), pp. 365–377. ISSN: 0935-9648. DOI: 10.1002/(sici)1521-4095(199803)10:5<365::aid-adma365>3.0.co;2-u.

[11] C. F. O. Graeff, R. M. Faria, F. E. G. Guimarães, and R. K. Onmori. "Field effect transistor using poly (o-metoxyaniline) films". In: (1999), pp. 151–153.

[12] S. Allard, M. Forster, B. Souharce, H. Thiem, and U. Scherf. "Organic semiconductors for solution-processable field-effect transistors (OFETs)". In: *Angewandte Chemie - International Edition* 47.22 (2008), pp. 4070–4098. ISSN: 14337851. DOI: 10.1002/anie.200701920.

[13] B. Kumar, B. K. Kaushik, and Y. S. Negi. "Organic Thin Film Transistors: Structures, Models, Materials, Fabrication, and Applications: A Review". In: *Polymer Reviews* 54.1 (2014), pp. 33–111. ISSN: 1558-3724. DOI: 10.1080/15583724.2013.848455.

[14] C. H. Kim, Y. Bonnassieux, and G. Horowitz. "Compact DC modeling of organic field-effect transistors: Review and perspectives". In: *IEEE Transactions on Electron Devices* 61.2 (2014), pp. 278–287. ISSN: 00189383. DOI: 10.1109/TED.2013.2281054.

[15] C. Liu, Y. Xu, and Y. Y. Noh. "Contact engineering in organic field-effect transistors". In: *Materials Today* 18.2 (2015), pp. 79–96. ISSN: 13697021. DOI: 10.1016/j.mattod.2014.08.037.

[16] A. Hepp, H. Heil, W. Weise, M. Ahles, R. Schmechel, and H. von Seggern. "Light-Emitting Field-Effect Transistor Based on a Tetracene Thin Film". In: *Physical Review Letters* 91.15 (2003), p. 157406. ISSN: 0031-9007. DOI: 10.1103/PhysRevLett.91.157406.

[17] E. C. P. Smits, S. Setayesh, T. D. Anthopoulos, M. Buechel, W. Nijssen, R. Coehoorn, P. W. M. Blom, B. De Boer, and D. M. De Leeuw. "Near-infrared light-emitting ambipolar organic field-effect transistors". In: *Advanced Materials* 19.5 (2007), pp. 734–738. ISSN: 09359648. DOI: 10.1002/adma.200600999.

[18] T. Sekitani, U. Zschieschang, H. Klauk, and T. Someya. "Flexible organic transistors and circuits with extreme bending stability." In: *Nature materials* 9.12 (2010), pp. 1015–1022. ISSN: 1476-1122. DOI: 10.1038/nmat2896.

[19] G. Gelinck, P. Heremans, K. Nomoto, and T. D. Anthopoulos. "Organic transistors in optical displays and microelectronic applications". In: *Advanced Materials* 22.34 (2010), pp. 3778–3798. ISSN: 09359648. DOI: 10.1002/adma.200903559.

[20] L. M. Dumitru, K. Manoli, M. Magliulo, G. Palazzo, and L. Torsi. "Low-voltage solid electrolyte-gated OFETs for gas sensing applications". In: *Microelectronics Journal* 45.12 (2014), pp. 1679–1683. ISSN: 00262692. DOI: 10.1016/j.mejo.2014.05.017.

[21] G. C. Faria, D. T. Duong, A Salleo, C. A. Polyzoidis, S Logothetidis, J Rivnay, R Owens, and G. G. Malliaras. "Organic electrochemical transistors as impedance biosensors". In: *Mrs Communications* 4.4 (2014), pp. 189–194. ISSN: 2159-6859. DOI: 10.1557/mrc.2014.35.

[22] V. Coropceanu, J. Cornil, D. A. da Silva Filho, Y. Olivier, R. Silbey, and J.-L. Brédas. "Charge transport in organic semiconductors". In: *Chem. Rev.* 107 (2007), pp. 926–952. ISSN: 03401022. DOI: 10.1007/128_2011_218.

[23] O. V. Mikhnenko, P. W. M. Blom, and T.-Q. Nguyen. "Exciton diffusion in organic semiconductors". In: *Energy Environ. Sci.* 8 (2015), pp. 1867–1888. ISSN: 1754-5692. DOI: 10.1039/c5ee00925a.

[24] C. Huang. "Organic Semiconductor for Flexible Electronics". PhD thesis.

[25] D. Alfredo and D. S. Pereira. "Control of a White Organic Light Emitting Diode ' s emission parameters using a single doped RGB active layer". In: September (2015). ISSN: 09215107. DOI: 10.1016/j.mseb.2016.07.004.

[26] D. Cibis. "Influencing Parameters in Droplet Formation for DoD Printing of Conductive Inks". In: *Proc. of the 4th Int. Conf. of Ceramic* (2008), pp. 417–423.

[27] M. Singh, H. M. Haverinen, P. Dhagat, and G. E. Jabbour. "Inkjet printing-process and its applications". In: *Advanced Materials* 22.6 (2010), pp. 673–685. ISSN: 09359648. DOI: 10.1002/adma.200901141.

[28] "Inkjet-printed line morphologies and temperature control of the coffee ring effect". In: *Langmuir* 24.5 (2008), pp. 2224–2231. ISSN: 07437463. DOI: 10.1021/la7026847.

[29] J. A. Lim, W. H. Lee, H. S. Lee, J. H. Lee, Y. D. Park, and K. Cho. "Self-organization of ink-jet-printed triisopropylsilylethynyl pentacene via evaporation-induced flows in a drying droplet". In: *Advanced Functional Materials* 18.2 (2008), pp. 229–234. ISSN: 1616301X. DOI: 10.1002/adfm.200700859.

[30] H. Li, G. Giri, J. B.-H. Tok, and Z. Bao. "Toward high-mobility organic field-effect transistors: Control of molecular packing and large-area fabrication of single-crystal-based devices". In: *MRS Bulletin* 38.01 (2013), pp. 34–42. ISSN: 1938-1425. DOI: doi:10.1557/mrs.2012.309.

[31] J. E. Anthony. *Research Interests of the Anthony Group*. URL: http://www.chem.uky.edu/research/Anthony/welcome.html (visited on 09/11/2016).

[32] Y. Y. Lin, D. J. Gundlach, S. F. Nelson, and T. N. Jackson. "Stacked pentacene layer organic thin-film transistors with improved characteristics". In: *IEEE Electron Device Letters* 18.12 (1997), pp. 606–608. ISSN: 07413106. DOI: 10.1109/55.644085.

[33] Z. Cui. *Printed Electronics: Materials, Technologies and Applications - Zheng Cui - Google Livros*. WILEY Higher Education Press, 2016.

[34] Z. Bao, J. Locklin, and G. Horowitz. *Organic field-effect transistors*. Vol. 10. 5. 2007, pp. 365–377. ISBN: 10: 0-8493-8080-4. DOI: 10.1002/(SICI)1521-4095(199803)10:5<365::AID-ADMA365>3.0.CO;2-U.

[35] Z. Stewart. "Organic Thin-Film Transistors and TIPS- Pentacene". In: *UKnowledge* (2013).

[36] J. E. Anthony. "The larger acenes: Versatile organic semiconductors". In: *Angewandte Chemie - International Edition* 47.3 (2008), pp. 452–483. ISSN: 14337851. DOI: 10.1002/anie.200604045.

[37] S. K. Park, D. A. Mourey, J. I. Han, J. E. Anthony, and T. N. Jackson. "Environmental and operational stability of solution-processed 6,13-bis(triisopropyl-silylethynyl) pentacene thin film transistors". In: *Organic Electronics: physics, materials, applications* 10.3 (2009), pp. 486–490. ISSN: 15661199. DOI: 10.1016/j.orgel.2009.02.007.

[38] Y. Yan, L. B. Huang, Y. Zhou, S. T. Han, L. Zhou, Q. Sun, J. Zhuang, H. Peng, H. Yan, and V. A. L. Roy. "Surface Decoration on Polymeric Gate Dielectrics for Flexible Organic Field-Effect Transistors via Hydroxylation and Subsequent Monolayer Self-Assembly". In: *ACS Applied Materials and Interfaces* 7.42 (2015), pp. 23464–23471. ISSN: 19448252. DOI: 10.1021/acsami.5b05363.

[39] Microdrop Technologies. "Autodrop compact micro dispensing system". 2014.

[40] X. Wang, M. Yuan, X. Xiong, M. Chen, M. Qin, L. Qiu, H. Lu, G. Zhang, G. Lv, and A. H. W. Choi. "Process optimization for inkjet printing of triisopropylsilylethynyl pentacene with single-solvent solutions". In: *Thin Solid Films* 578 (2015). ISSN: 00406090. DOI: 10.1016/j.tsf.2015.02.004.

[41] H. Klauk, M. Halik, U. Zschieschang, G. Schmid, W. Radlik, and W. Weber. "High-mobility polymer gate dielectric pentacene thin film transistors". In: *Journal of Applied Physics* 92.9 (2002), pp. 5259–5263. ISSN: 00218979. DOI: 10.1063/1.1511826.

[42] M. W. Lee, G. S. Ryu, Y. U. Lee, C. Pearson, M. C. Petty, and C. K. Song. "Control of droplet morphology for inkjet-printed TIPS-pentacene transistors". In: *Microelectronic Engineering* 95 (2012), pp. 1–4. ISSN: 01679317. DOI: 10.1016/j.mee.2012.01.006.

[43] C. Reese, M. Roberts, M.-m. Ling, and Z. Bao. *Organic Thin-Film Transistors (OTFTs)*. 2004.

[44] N. L. Vaklev, R. Miller, B. V. O. Muir, D. T. James, R. Pretot, P. Van Der Schaaf, J. Genoe, J. S. Kim, J. H. G. Steinke, and A. J. Campbell. "High-Performance Flexible Bottom-Gate Organic Field-Effect Transistors with Gravure Printed Thin Organic Dielectric". In: *Advanced Materials Interfaces* 1 (2014). ISSN: 21967350. DOI: 10.1002/admi.201300123.

[45] F. Gholamrezaie. "Self-assembled Monolayers in Organic Electronics". PhD thesis. University of Groningen, The Netherlands, 2012, p. 128. ISBN: 9789036756914.

[46] J. A. Lim, W. H. Lee, D. Kwak, and K. Cho. "Evaporation-Induced Self-Organization of Inkjet-Printed Organic Semiconductors on Surface-Modified Dielectrics for High-Performance Organic Transistors". In: *Langmuir* 25.9 (2009), pp. 5404–5410. ISSN: 07437463. DOI: 10.1021/la804269q.

[47] S.-I. Shin, J.-H. Kwon, H. Kang, and B.-K. Ju. "Solution-processed 6,13-bis(triisopropylsilylethynyl) (TIPS) pentacene thin-film transistors with a polymer dielectric on a flexible substrate". In: *Semiconductor Science and Technology* 23 (2008), p. 085009. ISSN: 0268-1242. DOI: 10.1088/0268-1242/23/8/085009.

[48] E. Tekin, B.-J. de Gans, and U. S. Schubert. "Ink-jet printing of polymers ? from single dots to thin film libraries". In: *Journal of Materials Chemistry* 14.17 (2004), p. 2627. ISSN: 0959-9428. DOI: 10.1039/b407478e.

[49] J. E. Anthony, J. S. Brooks, David L. Eaton, and S. R. Parkin. "Functionalized Pentacene: Improved Electronic Properties from Control of Solid-State Order". In: 222.11 (2001), pp. 9482–9483. DOI: 10.1021/JA0162459.

[50] J Zaumseil and H Sirringhaus. "Electron and Ambipolar Transport in Organic Field-Effect Transistors". In: *Chemical Reviews* 107 (2007), pp. 1296–1323. ISSN: 0009-2665. DOI: 10.1021/cr0501543.

Appendix A

Electrical Characterization of OFETs

The characterization of an OFET can be carried out by different electrical measurements. We can fix the gate voltage (V_G) and measure the drain-current (I_D) by sweeping the source-drain voltage (V_D). We can also fix a value for V_D in the linear regime and to trace the curve of I_D vs V_G, or to do the same for a drain voltage in the saturation regime. These curves are depicted in Figure A.1.

From the semilog plot (Figure A.1b) (in the linear regime) it is possible to extract the value for the subthreshold swing (S), which is an important parameter of an OFET, given by

$$S = \frac{\partial V_G}{\partial (log I_D)} \tag{A.1}$$

The subthreshold swing indicates how many gate volts are necessary to improve the drain current in one decade. From the I_D vs V_G curve one also can obtain the I_{ON}/I_{OFF} ratio, whose value corresponds to the performance of the transistor; i. e. higher the ratio, better the transistor will be. From the transfer characteristics in the saturation regime, on the other hand, one can extract the threshold voltage V_{th}. This value is directly obtained by extrapolating the linear dependence of the square root of the drain current with the gate voltage. Finally, as was mentioned in the section 1.1.1, we can calculate the value for the charge carrier mobility, in the saturation regime, by making use of the expression:

$$\mu_{OFET} = \frac{2L}{WC}\left(\frac{\partial \sqrt{I_D}}{\partial V_G}\right)^2 \tag{A.2}$$

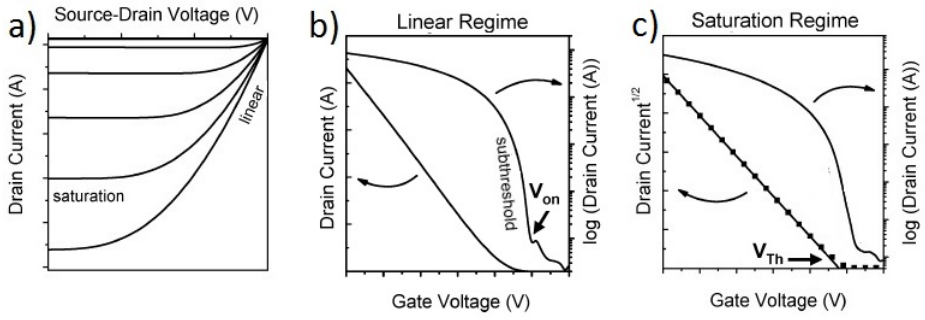

Figure A.1: Representative current-voltage characterisctics of an p-channel organic field-effect transistor. (a) output characteristics;(b) transfer characteristics in the linear regime indicating the onset voltage V_{on} when drain current increases suddenly; (c) transfer characteristics in the saturation regime indicating the threshold voltage V_{th}. This figure has adapted of the [50]